Available online at www.sciencedirect.com

SCIENCE DIRECT®

Tectonophysics 383 (2004) 217–241

TECTONOPHYSICS

www.elsevier.com/locate/tecto

Absence of a regional surface thermal high in the Baikal rift; new insights from detailed contouring of heat flow anomalies

Jeffrey Poort[a,*], Jan Klerkx[b,1]

[a] Free University Brussels (VUB), Pleinlaan 1030 Brussel, Belgium
[b] Department of Geology and Mineralogy, Royal Museum of Central Africa, Leuvensesteenweg 13, 3080 Tervuren, Belgium

Received 23 May 2003; accepted 25 March 2004

Abstract

Heat flow in active tectonic zones as the Baikal rift is a crucial parameter for evaluating deep anomalous structures and lithosphere evolution. Based on the interpretation of the existing datasets, the Baikal rift has been characterized in the past by either high heat flow, or moderately elevated heat flow, or even lacking a surface heat flow anomaly. We made an attempt to better constrain the geothermal picture by a detailed offshore contouring survey of known anomalies, and to estimate the importance of observed heat flow anomalies within the regional surface heat output. A total of about 200 new and close-spaced heat flow measurements were obtained in several selected study areas in the North Baikal Basin. With an outrigged and a violin-bow designed thermoprobe of 2–3-m length, both the sediment temperature and thermal conductivity were measured. The new data show at all investigated sites that the large heat flow highs are limited to local heat flow anomalies. The maximum measured heat flow reaches values of 300–35000 mW/m^2, but the extent of the anomalies is not larger than 2 to 4 km in diameter. Aside of these local anomalies, heat flow variations are restricted to near background values of 50–70 mW/m^2, except in the uplifted Academician zone. The extent of the local anomalies excludes a conductive source, and therefore heat transport by fluids must be considered. In a conceptual model where all bottom floor heat flow anomalies are the result of upflowing fluids along a conduit, an extra heat output of 20 MW (including advection) is estimated for all known anomalies in the North Baikal Basin. Relative to a basal heat flow of 55–65 mW/m^2, these estimations suggest an extra heat output in the northern Lake Baikal of only 5%, corresponding to a regional heat flow increase of 3 mW/m^2. The source of this heat can be fully attributed to a regional heat redistribution by topographically driven ground water flow. Thus, the surface heat flow is not expected to bear a signal of deeper lithospheric thermal anomalies that can be separated from heat flow typical for orogenically altered crust (40–70 mW/m^2). The new insights on the geothermal signature in the Baikal rift once more show that continental rifting is not by default characterized by high heat flow.

Keywords: Heat flow; Baikal rift; Offshore; Thermal anomalies; Vent model; Advection

1. Introduction

The Baikal rift belongs to continental rifts that are characterized by features such as a large water depth (up to 1640 m) and sedimentary infill (>10 km),

* Corresponding author. Present address: Renard Center of Marine Geology (RCMG), Universiteit of Ghent, Krijgslaan 281 S8, B-9000 Ghent, Belgium. Tel.: +32-9-264-45-90; fax: +32-9-264-4967.
E-mail addresses: jeffrey_poort@yahoo.com (J. Poort), jean.klerkx@pandora.be (J. Klerkx).
[1] Presently at: International Bureau for Environmental Studies (IBES), Audrey Hepburnstraat 9/13, 1090 Brussels, Belgium.

0040-1951/$ - see front matter © 2004 Elsevier B.V. All rights reserved.
doi:10.1016/j.tecto.2004.03.011

higher than expected strength and important crustal thinning variations (Déverchère et al., 1993; Burov et al., 1994). The Baikal rift also does not display an unambiguous elevated heat flow. Rifting features such as doming of the topography, negative P-wave velocity anomalies in the lithosphere, modest Cenozoic volcanics, and the presence of hydrothermal venting have led to suggestions that the thermal structure of the Baikal rift Zone is largely disturbed, but surface heat flow does not provide supporting evidence. Moreover, interpretation of the existing heat flow data has been highly inconsistent. The Baikal rift has been described as characterized by either high heat flow, or moderately elevated heat flow, or lacking a surface heat flow anomaly. This wide variation on the rift's thermal regime urges the need for a more detailed heat flow investigation integrating thermal measurements and modeling analysis. A better understanding of the observed heat flow variations and their origin is also of big importance to key issues in the current research of the energy-rich gas hydrate in Lake Baikal.

Many review articles have been published on the heat flow in the Baikal rift Zone (i.e., Lysak, 1978, 1984, 1995; Duchkov et al., 1999; Golubev, 2000). Several authors adopt a regional approach, including borehole data of the Baikal rift surrounding areas, and present large-scale interpretations. A focus on the rift area only offers a different challenge dealing with offshore heat flow mainly. A dataset of nearly 360 stations outlined the major features of the heat flow in Lake Baikal (Golubev et al., 1993). Heat flow in the basin averages to 71 ± 21 mW/m^2, but the basic feature is the highly unevenness of heat flow. In most parts of the basins, fluctuations of 30–40 mW/m^2 over distances of only several kilometers are occurring almost everywhere on the lake floor. This pattern of heat flow variability has also been demonstrated by heat flow maps derived indirectly from the depth of the Bottom Simulating Reflector or BSR (Golmshtok et al., 2000). More excessive heat flow anomalies with magnitudes of more than 200–1000 mW/m^2 have been observed along the basin border faults (Golubev, 1990). The site of highest heat flow was found in the northern basin in Frolikha Bay (Golubev, 1984) where a maximum value of 37 W/m^2 was measured (Crane et al., 1991). Hydrothermal discharge at the Frolikha anomaly (Golubev, 1984; Crane et al., 1991) suggests that thermal waters play a major role in the origin of the observed heat flow variability. The thermal waters appear to originate from an upper crustal circulation system involving meteoric water mainly (Polyak et al., 1992; Kipfer et al., 1996). Heat–fluid transport models show that a topographically driven groundwater circulation in the Baikal rift is able to redistribute heat towards the near-surface and to create enhanced heat output at basin boundaries (Golubev, 1990; Poort and Polyansky, 2002). The nature of the surface thermal anomalies is, however, still too poorly understood to quantify its contribution in the rift's thermal budget. In order to answer the question whether or not the surface heat flow picture in the Baikal rift reveals a signal from a large mantle thermal anomaly, a detailed study of the surface heat flow variability and its significance is needed.

In this paper, we present the results of a detailed heat flow mapping study in the northern Lake Baikal Basin. From 1993 to 1997, new and close-spaced heat flow measurements were obtained in several selected study areas. To the 360 heat flow data published in 1993, a total of about 200 new stations were added in the areas of Zavorotny, Frolikha, Hakusy, Academician Ridge, and along an axial transect of the North Baikal Basin. Initial results of the study, limited to the Zavorotny area, have been presented earlier (Golubev and Poort, 1995). We will show that in all studied areas, the large heat flow highs are limited to local heat flow anomalies only, not larger than 2 to 4 km in diameter. Aside of these local anomalies, heat flow variations are generally restricted to near background values of 50–70 mW/m^2. We further present a simple quantitative analysis of the conductive versus advective heat transport associated with the local heat flow anomalies, which will allow us to estimate the importance of the anomalies within the regional surface heat output.

2. Geological setting

Lake Baikal occupies the central part of the tectonically active Baikal rift Zone (Zonenshain et al., 1990; Logatchev, 1993) and is subdivided in the three sub-basins, the Southern (SBB), the Central (CBB) and the northern Baikal Basin (NBB) (Fig. 1). The NBB, to which the study area will be limited, has a maximum water depth of 900 m and is separated to south from the CBB by the underwater elevated block

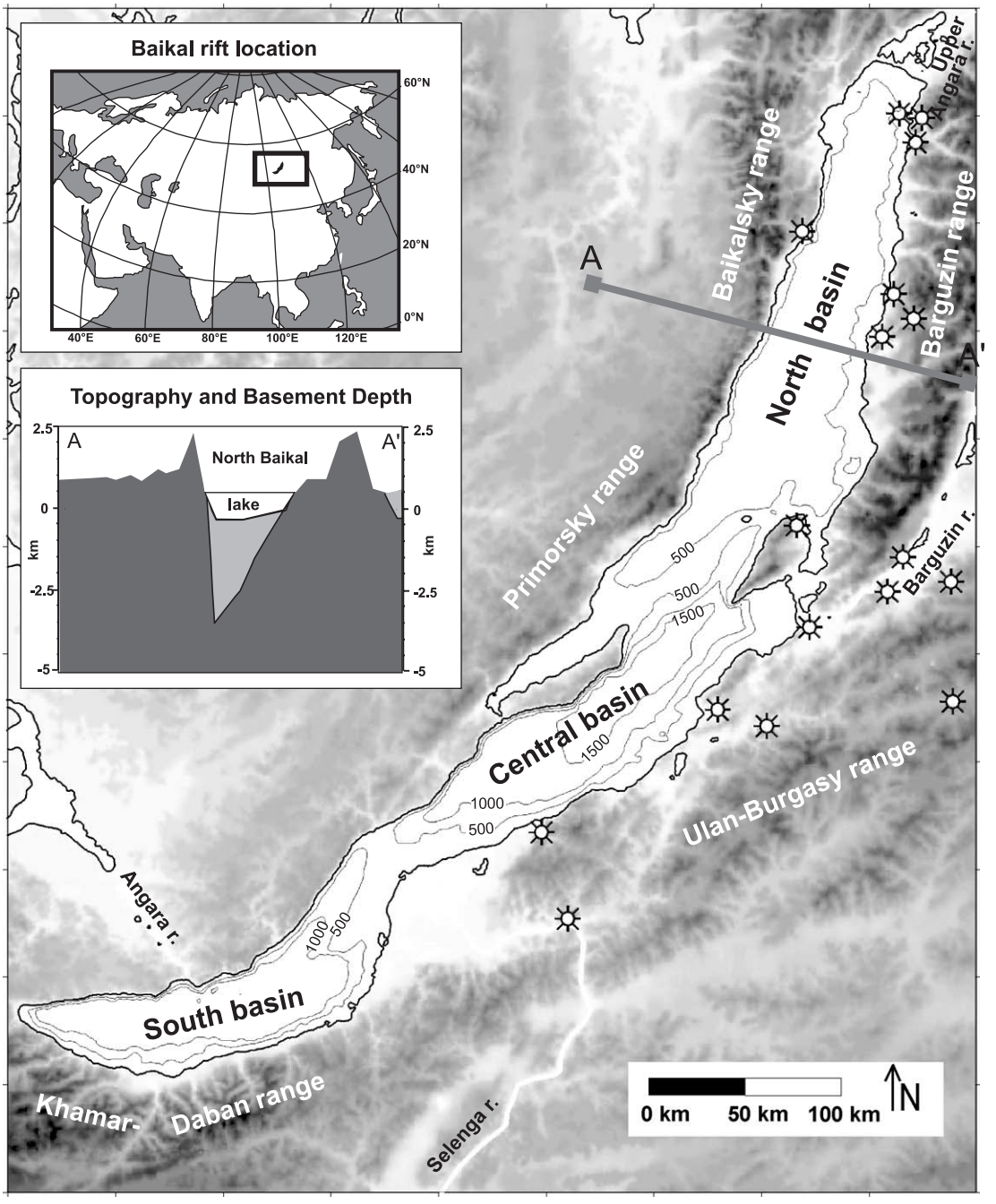

Fig. 1. Digital Elevation Model (DEM) of Lake Baikal Basins and the surrounding mountain ranges (modified from Delvaux et al., 2000) Also marked on the DEM are the on-land hot springs and the Frolikha off-shore vent (open stars). Insets show the location of the Baikal rift and a transect of the North Baikal Basin (NBB) along A – A′ illustrating uplifted flank topography, deep basin basement depth and lake water depth.

of Academician Ridge (AR) rising to a depth of about 300 m. The basin is bordered to the west and the east by mountain ranges of 1000 to 2500 m high. The lake itself is at 450 m above sea level (Fig. 1).

All basins are formed by subsidence along normal faults modified by oblique-slip and strike-slip tectonics, and exhibit an asymmetric, half-graben structure resulting in present-day drainages that are smaller on the western sides of the basin than on the ramp and axial margins (Hutchinson et al., 1992; Moore et al., 1997) (Fig. 1, inset). In the NBB, the sedimentary thickness is about 4 km and the Upper Angara River is the major source supplying sediments. The upper Holocene basin plain unit (1.4 to >4 m; Nelson et al., 1995) is mostly composed of diatom mud interbedded with thin turbidite layers, while the underlying glacial units are dominated by coarse silt or thick sand turbidites (Colman et al., 1998; Nelson et al., 1999). Sedimentation rate varies between 30 and 35 cm/ka in the NBB (Edgington et al., 1991; Colman et al., 1996) and only 4 cm/ka on the AR (Williams et al., 1997). The total sedimentary thickness in the NBB is about 4 km (Hutchinson et al., 1992). The high variety in structural and sedimentary environments undeniably has an important influence on the basin heat flow, and in particular on the advective part.

3. Existing thermal data

In the on-shore rift zone region surrounding Lake Baikal, relatively poor and uneven distributed coverage of heat flow determinations exists for the rift zone area (Fig. 2, inset). Measurements were made in exploratory drill holes ranging generally from 0.5 to 1.5 km in depth and returned heat flow values ranging from 18 to 150 mW/m^2 (Lysak, 1995). Heat flows exceeding 80 mW/m^2 are connected to border fault systems where thermal waters are interfering with heat dissipation, while in the uplifted rift flanks heat flow averages to a lower value of about 40 mW/m^2. To make any conclusive interpretation on the rift heat flow, the on-land heat flow is too sparsely sampled. Offshore, on the other hand, a large heat flow dataset provides a much better base for a detailed analysis of the basin heat flow. Heat flow in Lake Baikal has been collected for more than 35 years now (Lyubimova and Shelyagin, 1966; Lubimova, 1969; Duchkov et al., 1976, 1979; Golubev, 1978, 1982, 1987, 1995; Golubev and Osokina, 1980), with the major heat flow features outlined by the numerous measurements performed by Golubev.

From the 360 heat flow data from Lake Baikal that were published up to 1993, 200 of the stations were made in the NBB and Academician Ridge, the areas of fieldwork investigations within this study (Fig. 2). This dataset shows in the NBB a heat flow that generally ranges between 50 and 70 mW/m^2, but with excessively low and high values along both shores and moderately elevated heat flow in northern and southern (Academician Ridge) terminations of the basin. The high heat flow anomalies along the shores of the North Basin are by far the most striking thermal features of the rift basin: a total of nine spots with heat flow values higher than 150 mW/m^2 and up to several thousands of mW/m^2 are documented (Golubev, 1995). Along the east side of the NBB high heat flow anomalies has been found in six offshore locations at water depths of 300–500 m. Highest heat flow values have been measured in the Frolikha hydrothermal vent (35 W/m^2) and in the Hakusy area 15 km south of it (2,1 W/m^2). Both sites are associated with on-land springs where thermal water is discharging at a rate of 5–50 l/s and with a temperature of 35–46 °C (Pinneker and Lomonosov, 1973). The other heat flow highs along the eastern basin side have magnitudes ranging from 159 to 1023 W/m^2. Along the steep western basin border, two sites have been discovered off-shore Zavorotny in a 40-km-long relay ramp between overstepping faults. Heat flow maxima of 999 and 450 mW/m^2 were measured, respectively, at depths of 350 and 900 m. More northwards along the steep slope, a heat flow of 240 mW/m^2 is registrated off-shore Baikalskoe at a water depth of more than 700 m. None of the west side anomalies are close to on-land thermal vents, but all occur where the simple single slope structure at the western border turns in a more complex structural transition zone.

The heat flow anomalies outlined by the existing heat flow dataset offer a unique basis for a more detailed investigation of the different types of anomalies. The existing data generally do not allow to confidently map the extent of the anomaly, in particular in the direction parallel to the rift. Additional heat flow measurement will allow to contour in detail the known heat flow anomalies and to produce heat flow

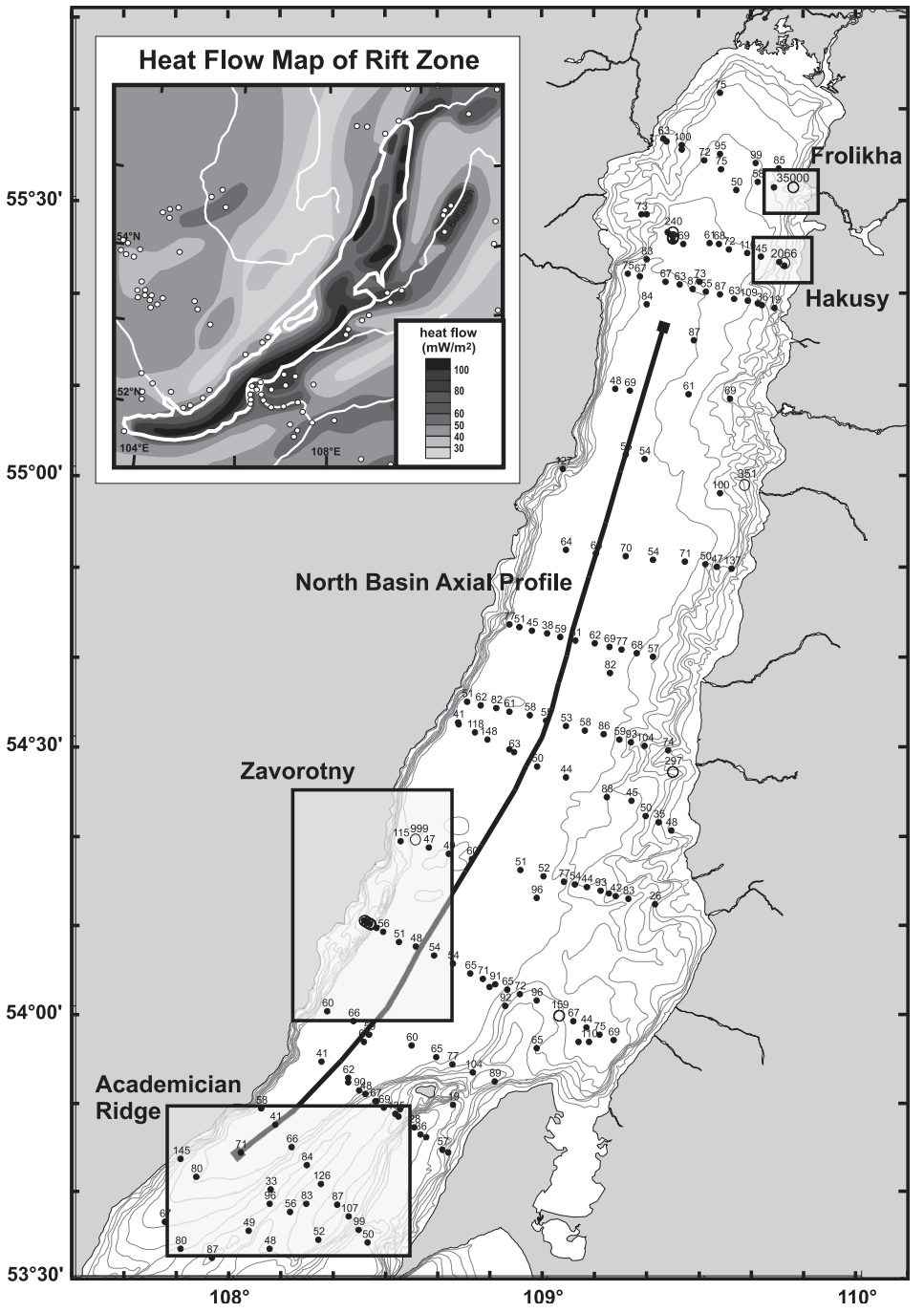

Fig. 2. Geothermal stations with heat flow values (mW/m^2) made in North Baikal Basin prior to the new data (see text). The frames show the areas chosen for new, detailed heat flow investigations. Inset: Map of the heat flow in the Baikal rift and surrounding area. Off-shore heat flow contours are redrawn from Golubev et al. (1993) and on-land contours redrawn from the published map of Lysak (1995). White dots are the heat flow measurement sites in the drillholes on-land.

density maps of the anomalous regions. These maps will help to further study (1) the source and the nature of the different rift heat flow anomalies, (2) the conductive versus convective heat output at the anomalies, and (3) to make a more accurate thermal balance of the rift.

4. Data acquisition and methods

4.1. Technique

New heat flow measurements were obtained from 1993 to 1997, using two different thermoprobes of 2–3 m in length: the probe constructed by Golubev and the GEOS-T. The "Golubev" probe (Golubev, 1987) is configurated with several outrigged sensors according to the Ewing technique. Each outrigger (about 12 cm in length, 4 mm in diameter) is used as temperature sensor and conductivity needle probe. This device has been used by Golubev for geothermal work on Lake Baikal for the last 20 years. The GEOS-T thermoprobe, developed by PALS (Samara, Russia), is constructed according to the violin-bow design, with two separate full-length outrigged probes connected to the central lance. One probe is used for thermal gradient measurement and consists of five thermistors equally spaced at half-meter intervals. The other probe measures in-situ thermal conductivity and contains a linear heat element in combination with four grouped thermistors. This construction allows to obtain both thermal gradient and conductivity over the same depth interval. Real-time monitoring during probe lowering allows controlling of instrument performance and data quality. After penetration into the sediments, the probe is left undisturbed for 15–20 min, with the conductivity measurement starting after about 5 min. All geothermal data (including temperature of thermistor probes, near-bottom-water temperature, tilt, pressure) are logged at 2.5-s intervals. Failures and incomplete penetrations due to hard substrate occurred several times, but were easily evaluated.

The thermal gradient is determined using thermistor temperatures extrapolated to equilibrium. Equilibrium temperatures have an uncertainty of less than 1 mK. Instrumental error on the thermal gradient is between 1% and 5%. At most stations, the thermal gradient decreased slightly with depth. This trend is normal in the upper m of the sediments where compaction results in increasing thermal conductivity with depth. At each station, average thermal gradient and standard deviation are calculated. At some stations, a strong break is observed. In that case, the thermal gradient is rejected or calculated with a reduced amount of equilibrium temperature. In situ thermal conductivity is measured using the continuous heating technique (as in Lister, 1970). Instrumental error on each determination is about 5%. As shown in Fig. 3, thermal conductivity generally increases with depth, from around 0.8–0.9 W/m K at the surface up to 0.9–1.1 W/m K at 2-m depth. The reported thermal conductivity at each station is the harmonic mean of the individual determinations. Stations with signs of probe leakage were rejected and thermal conductivity of nearby stations was used for heat flow calculations. Heat flow values were computed for each depth interval as the product of the thermal gradient and thermal conductivity, and then averaged. The instrumental error on the calculated heat flow is 10% and standard deviations are generally within this range. The calculated thermal gradients, thermal conductivities and heat flow data are summarized in Table 1. It should be noted that for the first time stations were positioned with GPS accuracy. Positioning of the previous heat flow data in Lake Baikal was based on landmarks only (capes, mountains and river outlets) with absolute and relative position limited to an accuracy of about 100–500 m.

4.2. Particular conductivity features of a lacustrine environment

The lacustrine sedimentary environment, in particular in large lakes such as Baikal, includes with terrigenous sediments such as turbidites and glacial deposits, and has a diversity in sedimentary environments which is usually not found in oceanic areas. In the NBB, three major depositional areas are distinguished (Colman et al., 1998): (1) the basin floor and subaqueous fans, which constitute the vast majority of the basin area, (2) the bathymetric high of Academician Ridge in the south, and (3) the large Upper Angara delta in the north. Turbidite systems dominate in basin floor and subaqueous fans, where diatomaceous muds and massive clays are interbedded for 7–21 % by coarse silt to sand turbidite layers of 3–7 cm.

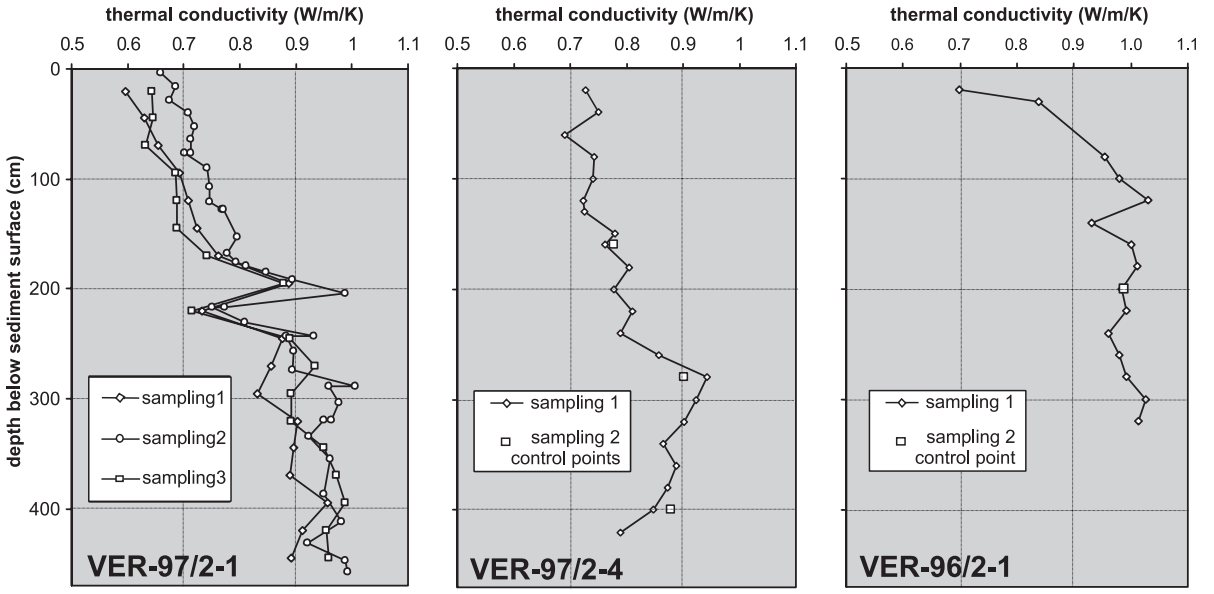

Fig. 3. Variation of the thermal conductivity with depth: data from needle probe measurements on three sediment cores (two from the Central basin and one in the Hakusy area).

(Sturm et al., 1998; Nelson et al., 1999). In these turbidite-dominated sediments, it can be expected to encounter a high thermal conductivity variability, both vertically and laterally and with values ranging between 0.7 and 1.3 W/m K (e.g., Louden et al., 1987; Jemsek and Von Herzen, 1989; Davis and Seemann, 1994). The conductivity in turbidite rich regions will have a stronger influence on the variations in heat flow compared to the deep ocean. Therefore, a good sampling of the thermal conductivity structure of the upper sediments is important.

Vertical variability of the thermal conductivity in the upper meters of the sediment at the west side of the NBB (Zavorotny area) was studied in-situ using a 3-m-long thermoprobe (Golubev and Poort, 1995). Measurements at 19 stations returned averaged thermal conductivities of 0.72, 0.91, 1.00, and 1.08 W/m K for, respectively, 0, 1, 2 and 3 m below the sediment surface. Although there is a general trend of increasing conductivity with depth, at several stations, maximum conductivity is reached at intermittent levels. The vertical variability was studied in more detail on sediment samples on board of the ship using the LITOS needle probe (Poort, 2000). Thermal conductivity was measured at depth intervals of not more than 10–20 cm and showed the same trend of a general increasing conductivity with local intermediate peaks (Fig. 3). From a depth of 1 to 3 m onwards, the thermal conductivity general ranges between 0.9 and 1.0 W/m K, which is in good agreement with the in-situ data.

Information on the lateral variability can be obtained on a statistical basis using both old and new data about the thermal conductivity of the different sedimentary environments. In the axial part of the basins (in particular for the NBB), the thermal conductivity of sediments at 1–2 m averages to 0.92 W/m K. Near the basin flanks, where the sedimentary environment consists of alluvial fans, aprons, and glacial outwash-fans, conductivity is higher and more variable, most probably between 0.9 and 1.1 W/m K. For the bathymetric high of Academician Ridge, only a few reliable estimates of conductivity are available. These data suggest a value around 0.9 W/m K.

4.3. Environmental factors to be considered

In addition to the instrumental error, heat flow measurements are sensitive to a number of geological and hydrological factors, e.g., sedimentation, lake-floor topography and dipping, bottom-water instability, heat refraction, erosion, etc. Especially in the upper part of the sedimentary column, these environ-

Table 1
Heat flow data acquired in Lake Baikal during several expeditions from 1993 to 1997

Number	Station name	Y	Coordinates				WD (m)	PP (m)	GR (mK/m)	TC (W/m K)	HF (mW/m^2)
			North°	min	West°	min					
Zavorotny area											
1	HFZA9301	93	54	16.86	108	33.82	743	2	77	0.99	76
2	HFZA9302	93	54	17.38	108	33.17	646	2	37	1.07	40
3	HFZA9303	93	54	18.43	108	34.78	761	2	94	1.00	94
4	HFZA9304	93	54	18.52	108	36.10	837	2	91	0.94	85
5	HFZA9305	93	54	16.23	108	35.57	790	2	210	1.07	225
6	HFZA9306	93	54	17.65	108	35.53	790	2	227	1.06	240
7	HFZA9307	93	54	16.93	108	34.81	818	2	388	0.99	385
8	HFZA9308	93	54	16.23	108	33.96	818	2	92	0.65	60
9	HFZA9309	93	54	15.15	108	33.48	818	2	57	0.70	40
10	HFZA9310	93	54	14.58	108	30.30	423	2	153	1.10	168
11	HFZA9311	93	54	15.31	108	30.57	498	2	74	1.03	76
12	HFZA9312	93	54	16.02	108	31.28	489	2	71	0.94	66
13	HFZA9313	93	54	17.80	108	34.80	808	2	215	1.05	226
14	HFZA9314	93	54	18.20	108	34.90	714	2	184	1.00	184
15	HFZA9315	93	54	16.60	108	34.50	771	2	212	0.90	190
16	HFZA9316	93	54	19.50	108	38.00	667	2	197	0.62	121
17	HFZA9317	93	54	20.60	108	30.80	705	2	111	1.13	125
18	HFZA9318	93	54	21.58	108	33.34	714	2	82	1.00	82
19	HFZA9319	93	54	16.37	108	35.29	818	2	88	0.89	78
20	HFZA9320	93	54	16.75	108	34.98	818	2	141	0.73	104
21	HFZA9321	93	54	16.99	108	35.09	818	2	306	0.88	271
22	HFZA9322	93	54	17.44	108	35.05	785	2	249	0.98	245
23	HFZA9323	93	54	17.61	108	34.67	667	2	229	0.94	215
24	HFZA9324	93	54	17.28	108	34.48	743	2	234	0.84	196
25	HFZA9325	93	54	17.24	108	35.87	818	2	175	0.87	152
26	HFZA9326	93	54	14.37	108	31.28	414	2	80	0.92	73
27	HFZA9327	93	54	14.51	108	29.80	404	2	388	0.99	384
28	HFZA9328	93	54	14.52	108	29.22	470	2	100	0.94	94
29	HFZA9401	94	54	2.66	108	30.74	870	3	55	0.94	50
30	HFZA9402	94	54	4.57	108	25.47	879	3	58	0.96	55
31	HFZA9403	94	54	5.50	108	22.87	874	3	68	1.14	78
32	HFZA9404	94	54	5.86	108	21.46	451	2	68	0.90	62
33	HFZA9407	94	54	11.01	108	35.69	884	3	46	0.87	40
34	HFZA9408	94	54	11.74	108	31.19	874	3	131	1.03	135
35	HFZA9409	94	54	12.36	108	28.75	465	2	55	0.91	50
36	HFZA9410	94	54	12.43	108	27.61	437	2	60	1.00	61
37	HFZA9413	94	54	10.08	108	25.15	348	2	73	0.95	70
38	HFZA9414	94	54	9.59	108	26.42	503	2	46	0.88	40
39	HFZA9415	94	54	9.07	108	27.65	874	3	124	1.09	135
40	HFZA9417	94	54	9.06	108	23.35	240	3	47	1.08	50
41	HFZA9419	94	54	8.98	108	28.08	874	3	87	1.02	88
42	HFZA9420	94	54	9.03	108	27.25	827	2	134	0.96	129
43	HFZA9421	94	54	9.49	108	27.06	649	3	60	1.01	60
44	HFZA9422	94	54	9.56	108	26.12	456	2	55	0.92	50
45	HFZA9424	94	54	10.76	108	27.26	588	1	65	0.95	62
46	HFZA9427	94	54	14.53	108	30.08	437	2	127	0.96	122
47	HFZA9428	94	54	14.54	108	29.73	437	2	383	1.04	397
48	HFZA9429	94	54	14.32	108	28.81	494	2	78	0.99	76
49	HFZA9430	94	54	14.66	108	28.84	498	3	75	1.01	75
50	HFZA9431	94	54	14.15	108	29.85	414	2	89	1.05	94
51	HFZA9434	94	54	6.29	108	24.08	874	3	101	1.08	108

Table 1 (*continued*)

Number	Station name	Y	Coordinates				WD (m)	PP (m)	GR (mK/m)	TC (W/m K)	HF (mW/m^2)
			North°	min	West°	min					
Zavorotny area											
52	HFZA9435	94	54	6.65	108	25.14	874	3	61	1.03	63
53	HFZA9436	94	54	7.48	108	25.41	846	3	94	1.08	101
54	HFZA9437	94	54	7.88	108	26.30	846	2	75	0.97	73
55	HFZA9440	94	54	9.62	108	28.12	874	2	92	0.96	88
56	HFZA9441	94	54	9.86	108	28.85	879	3	59	0.96	56
57	HFZA9442	94	54	10.36	108	29.70	874	1	39	1.13	44
58	HFZA9443	94	54	8.85	108	24.04	259	2	136	0.95	128
59	HFZA9444	94	54	9.46	108	24.77	296	2	311	0.90	279
60	HFZA9449	94	54	19.00	108	34.56	799	2	99	1.16	116
61	HFZA9451	94	54	19.23	108	36.58	771	3	55	1.12	61
62	HFZA9452	94	54	17.88	108	37.20	855	2	73	1.12	81
63	HFZA9455	94	54	11.10	108	30.25	874	1	37	1.03	38
64	HFZA9456	94	54	12.51	108	31.52	874	3	73	1.25	91
65	HFZA9457	94	54	13.07	108	32.00	846	3	64	1.10	71
66	HFZA9458	94	54	14.19	108	33.05	879	3	47	0.94	44
67	HFZA9459	94	54	19.81	108	32.48	752	3	110	1.03	114
68	HFZA9460	94	54	21.99	108	33.88	799	3	75	1.00	75
69	HFZA95g1	95	54	19.73	108	35.00	790	3	88	–	88
70	HFZA95g2	95	54	18.56	108	34.35	790	3	104	–	104
71	HFZA95g3	95	54	16.30	108	36.82	884	2	64	–	64
72	HFZA95g4	95	54	15.15	108	34.66	882	2	57	–	57
73	HFZA95g5	95	54	12.40	108	31.37	879	2	82	–	82
74	HFZA95g6	95	54	8.27	108	26.89	876	3	74	–	74
75	HFZA95g7	95	54	13.17	108	33.76	879	3	78	–	78
76	HFZA9502	95	54	0.35	108	17.53	812	2	77	–	77
77	HFZA9503	95	54	3.08	108	21.14	871	2	79	–	79
78	HFZA9504	95	54	2.08	108	23.27	876	2	73	–	73
79	HFZA9505	95	54	0.31	108	29.34	874	2	67	–	67
80	HFZA9506	95	54	9.45	108	24.82	291	2	800	–	800
81	HFZA9507	95	54	10.61	108	30.30	874	2	61	–	61
82	HFZA9508	95	54	14.18	108	37.10	881	2	59	–	59
83	HFZA9509	95	54	17.26	108	34.66	836	2	545	–	545
84	HFZA9510	95	54	22.18	108	37.28	836	2	71	–	71
Frolikha area											
1	HFFR9512	95	55	31.23	109	43.12	446	1.5	78	–	78
2	HFFR9514	95	55	32.62	109	45.86	427	1.5	90	–	90
3	HFFR9515	95	55	32.18	109	46.78	395	2	82	–	82
Hakusy area											
1	HFHA9601	96	55	24.68	109	46.10	420	2	60	–	60
2	HFHA9602	96	55	24.08	109	45.82	409	2	76	1.03	78
3	HFHA9603	96	55	23.41	109	45.90	353	2	129	1.06	137
4	HFHA9604	96	55	22.96	109	45.85	244	2	226	–	226
5	HFHA9605	96	55	22.21	109	45.90	194	2	110	–	110
6	HFHA9606	96	55	21.53	109	45.57	244	2	88	0.94	83
7	HFHA9607	96	55	20.53	109	45.21	212	2	89	–	89
8	HFHA9608	96	55	20.43	109	42.85	498	2	45	–	45
9	HFHA9609	96	55	21.90	109	43.05	410	1.5	37	–	37
10	HFHA9610	96	55	22.36	109	47.07	136	1.5	107	–	107
11	HFHA9611	96	55	23.11	109	46.82	234	2	903	–	903

(continued on next page)

Table 1 (*continued*)

Number	Station name	Y	Coordinates				WD (m)	PP (m)	GR (mK/m)	TC (W/m K)	HF (mW/m^2)
			North° min		West° min						
Hakusy area											
12	HFHA9612	96	55	23.66	109	47.10	264	2	87	–	87
13	HFHA9613	96	55	23.35	109	44.76	392	2	199	–	199
14	HFHA9614	96	55	23.20	109	45.36	296	2	145	–	145
15	HFHA9615	96	55	22.62	109	44.83	358	2	81	–	81
16	HFHA9616	96	55	23.03	109	43.52	571	1	56	–	56
17	HFHA9617	96	55	23.78	109	43.61	525	2	55	1.10	60
18	HFHA9618	96	55	24.70	109	44.58	536	2	93	1.12	104
19	HFHA9619	96	55	23.76	109	45.07	429	2	118	–	118
20	HFHA9620	96	55	23.22	109	46.40	308	2	409	–	409
21	HFHA9621	96	55	22.82	109	45.26	314	2	114	–	114
22	HFHA9622	96	55	23.43	109	38.79	714	2	73	–	73
23	HFHA9623	96	55	25.30	109	43.60	601	2	87	–	87
24	HFHA9624	96	55	23.52	109	45.48	389	2	131	–	131
25	HFHA9625	96	55	27.10	109	46.01	470	2	150	–	150
26	HFHA9626	96	55	23.40	109	46.54	305	2	157	–	157
27	HFHA9627	96	55	23.10	109	44.65	416	2	138	1.08	149
28	HFHA9628	96	55	20.00	109	44.33	428	2	31	–	31
Academician Ridge area											
1	HFAC9401	94	53	38.61	108	9.11	378	3	121	0.89	108
2	HFAC9402	94	53	39.24	108	9.20	380	3	67	–	60
3	HFAC9403	94	53	39.67	108	14.49	398	3	111	0.93	103
1	HFAC9501	95	53	29.39	107	41.14	425	2	73	–	73
1	HFAC9601	96	53	31.52	108	15.23	742	2	123	–	113
2	HFAC9602	96	53	35.60	108	10.52	430	2	61	–	55
3	HFAC9603	96	53	37.27	108	7.07	360	2	85	–	77
4	HFAC9604	96	53	37.94	108	8.17	361	2	75	–	68
5	HFAC9605	96	53	38.99	108	8.91	372	2	79	–	71
6	HFAC9606	96	53	39.85	108	10.16	366	2	87	–	78
7	HFAC9607	96	53	40.34	108	11.35	369	2	90	–	81
8	HFAC9608	96	53	40.70	108	12.35	357	2	77	–	69
9	HFAC9610	96	53	42.90	108	16.90	417	2	89	–	80
10	HFAC9611	96	53	41.43	108	18.72	352	2	93	–	84
11	HFAC9612	96	53	38.93	108	4.01	494	2	72	–	65
12	HFAC9613	96	53	36.08	108	8.52	482	2	65	–	59
13	HFAC9614	96	53	36.19	108	5.51	363	2	96	–	86
14	HFAC9615	96	53	35.10	108	4.23	311	2	66	–	59
15	HFAC9616	96	53	34.74	108	2.61	312	2	62	–	56
16	HFAC9617	96	53	34.50	108	1.40	282	2	91	–	82
17	HFAC9618	96	53	33.95	108	0.64	287	2	89	–	80
18	HFAC9619	96	53	32.58	107	57.42	294	2	76	–	68
19	HFAC9620	96	53	36.70	108	7.45	512	2	119	–	107
20	HFAC9622	96	53	38.42	108	5.22	417	2	70	–	63
21	HFAC9623	96	53	40.70	108	1.92	732	2	62	–	56
22	HFAC9624	96	53	39.40	108	7.85	446	2	85	–	77
23	HFAC9625	96	53	38.45	108	7.85	351	2	83	–	75
24	HFAC9626	96	53	44.90	108	10.20	859	2	67	–	62
25	HFAC9627	96	53	42.75	108	12.95	411	2	81	–	73
26	HFAC9628	96	53	41.11	108	15.14	391	2	111	–	100
27	HFAC9629	96	53	40.14	108	16.57	348	2	119	–	107
28	HFAC9630	96	53	39.30	108	18.01	322	2	109	–	98
29	HFAC9631	96	53	38.15	108	18.60	274	2	88	–	79

Table 1 (*continued*)

Number	Station name	Y	Coordinates				WD (m)	PP (m)	GR (mK/m)	TC (W/m K)	HF (mW/m^2)
			North°	min	West°	min					
Academician Ridge area											
30	HFAC9632	96	53	38.33	108	16.06	339	2	95	–	86
31	HFAC9701	97	53	39.15	108	14.10	379	2	113	–	102
32	HFAC9702	97	53	37.97	108	11.56	444	2	61	–	55
33	HFAC9703	97	53	35.70	108	14.63	329	2	69	–	62
34	HFAC9704	97	53	33.35	108	13.10	351	2	57	–	51
North axial profile											
1	HFNA9701	97	53	43.70	108	1.84	849	2	92	–	85
2	HFNA9725	97	53	45.15	108	4.99	861	2	76	–	70
3	HFNA9702	97	53	48.51	108	12.25	877	2	63	–	58
4	HFNA9703	97	53	53.90	108	21.16	873	2	67	–	62
5	HFNA9704	97	53	59.98	108	29.89	874	2	69	–	63
6	HFNA9705	97	54	3.00	108	32.88	876	2	64	–	59
7	HFNA9706	97	54	6.35	108	35.95	879	2	62	–	57
8	HFNA9707	97	54	9.14	108	38.87	878	2	64	–	59
9	HFNA9709	97	54	14.98	108	45.07	878	2	65	–	60
10	HFNA9710	97	54	17.98	108	48.04	876	1.5	77	–	71
11	HFNA9712	97	54	24.12	108	54.60	871	2	79	–	73
12	HFNA9713	97	54	26.70	108	56.61	870	1.5	61	–	56
13	HFNA9714	97	54	29.90	108	59.60	874	2	68	–	63
14	HFNA9715	97	54	33.30	109	1.60	876	2	62	–	57
15	HFNA9716	97	54	35.90	109	2.71	876	2	72	–	66
16	HFNA9717	97	54	38.91	109	4.35	875	2	75	–	69
17	HFNA9718	97	54	41.90	109	5.55	874	2	81	–	75
18	HFNA9720	97	54	47.79	109	8.64	870	1.5	87	–	80
19	HFNA9721	97	54	53.99	109	11.95	863	2	70	–	64
20	HFNA9722	97	54	59.58	109	14.65	852	2	60	–	55
21	HFNA9724	97	55	15.68	109	22.80	805	2	93	–	86

Y = year of expedition, WD = water depth, PP = probe penetration, GR = measured geothermal gradient, TC = harmonic mean of in situ thermal conductivity, HF = calculated averaged heat flow value (where thermal conductivity measurement failed, average value for the specific sedimentary environment is taken. See text for more explanation).

mental effects can alter the measured heat flow values significantly. Hence, the data coming from the 2-m thermoprobe have to be interpreted with caution. Corrections for topography and sedimentation using simplified models (Lachenbruch, 1968; Von Herzen and Uyenda, 1963) are estimated to be in most places less than −10% to 10% of the measured values. Regional topography will result in an elevation of the heat flow in the basin (2–10%) and a reduction on the Academician Ridge (maximum 4%). Larger anomalies can be generated by local relief structures and within 1 km near the steep western slope. A constant sedimentation of 0.03 cm/year since the onset of formation of the NNB (5 Ma) will theoretically increase the heat flow up to 18% in the deep basin, but a correction of half this value is assumed to be more appropriate for the real sedimentation environment. The effect of sedimentation is much smaller on the eastern side of the lake and negligible on Academician Ridge. In table and maps, we present heat flow data that are not corrected for environmental processes because the application of a correction using simple models and poorly known parameters might bias the heat flow towards "less correct" values (e.g., Lounden and Wright, 1989).

Also, seasonal bottom-water temperature variations should be taken into account, since they can affect geothermal gradient values, and hence heat flow. Despite the theoretical stable stratification of the water column below 250 m, it has been evidenced that deep water circulation occurs (Weiss et al., 1991) due to the disturbance by external

physical mechanisms, such as wind shear (Shimaraev et al., 1993), salinity differences between the basins (Hohmann et al., 1997), and saline hydrothermal water input (Kipfer et al., 1996). CTD data from the Zavorotny area suggest temperature variations of only 0.013 °C at a depth of 920 m. Such differences can affect the measured heat flow for not more than 1% (Lounden and Wright, 1989; Poort, 2000). In the Frolikha study area, which is located at a shallow depth, a difference of 0.03 °C is recorded between station depths of 600 and 300 m, and 0.1 °C between 600 and 250 m. Unfortunately, we do not have information on the variations with time needed to estimate the effect on the heat flow measurements.

5. The heat flow anomalies

Within Lake Baikal, the NBB has the highest density of existing heat flow stations and exhibits the strongest surface heat flow anomalies found in the lake. The sites of high heat flow in North Baikal were discussed in paragraph 3, the new observations and insights will be discussed here. Close-spaced heat flow measurements were obtained in four selected study areas (Fig. 2): Zavorotny on the west side, Frolikha and Hakusy on the east side, and Academician Ridge south of the NBB. In addition to the high heat flow sites of study, a transect of new heat flow measurements was performed along the axis of the NBB in order to compare the high heat flow sites with variation in the background heat flow.

5.1. The Zavorotny anomalies

The Zavorotny study area covers a zone of 40 by 15 km featuring a relay ramp between an overstepping fault system (Delvaux et al., 2000). In this area, a total of 84 new geothermal stations were added to the 14 existing stations (Table 1). The majority of the new stations were obtained in 1993 and 1994, and preliminary discussed by Golubev and Poort (1995). In 1995, nine more stations were collected using the GEOS-T probe, basically for additional background values and defining the intensity of the anomaly intensity.

The Zavorotny heat flow map presented in Fig. 4 is contoured using the minimum curvature gridding method. It clearly outlines three areas with a different heat flow picture. A background heat flow of about 50–70 mW/m^2 is found on the lake floor at a distance from the slope. At the base of the steep slope, heat flow is much more variable, from low values of 35 mW/m^2 to moderate high heat flow of 130 mW/m^2. The zone of strong positive heat flow anomalies (>400 mW/m^2) is located on the basement high and the northern end of it. Three anomalies are situated 10 km apart from each other and are clearly separated by zones of background heat flow. The previously known northern and southern anomalies reach heat flow maxima of 800–1000 mW/m^2, where the newly discovered heat flow high in between reaches 400 mW/m^2. The extent of all three anomalies turns out to be limited in all directions, with a diameter of 2–4 km for the 150-mW/m^2 contour. In most directions, the diameter of the contour of 65 mW/m^2 (background heat flow) is not more than 3–6 km.

The northern anomaly is located where the underwater fault scarp dies out into the flat lake floor. This anomaly is contoured in detail and shows an orientation of the long axis in NNE direction. The two other anomalous heat flow areas are at smaller bathymetric depths, both located close to a north tip of ridge-like structures bounding the basement high. The nature of the thermal anomalies appears to be closely linked to the tectonic setting, with the relay ramp providing pathways for increased heat flow.

5.2. The Frolikha anomaly

The Frolikha study area is limited by 5 to 7 km, encircling the known hydrothermal vent. Just northwest of the vent center, the area features a local morphological high interpreted as a single-levee (Back et al., 1999). Three new stations were added to the seven previously known stations (Table 1) and thirteen previously unpublished stations were incorporated. Many parts of the study area turned out to be impossible to penetrate with a two-meter probe, in particular southwards of the vent center.

In Fig. 5 the shape and extent of the Frolikha thermal anomaly is contoured manually. The center of the anomaly corresponds to the venting area. Three heat flow maxima (37, 20, and 9 W/m^2) measured at the center are slightly offset to each other. The offsets can be real, but can also be explained as the result of

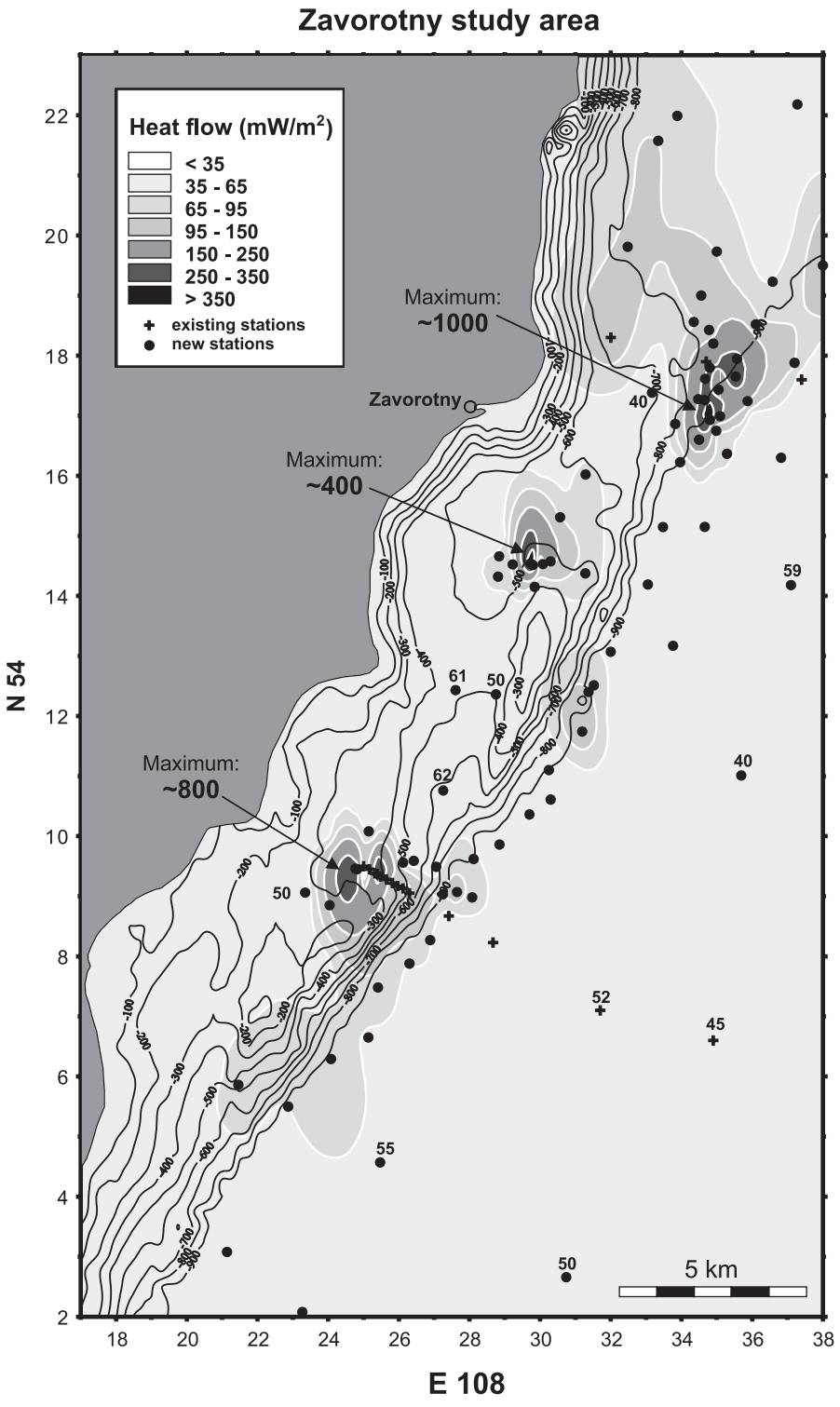

Fig. 4. Heat flow contour map in the Zavorotny area, based on existing stations (Golubev, 1982, 1995) and new geothermal stations.

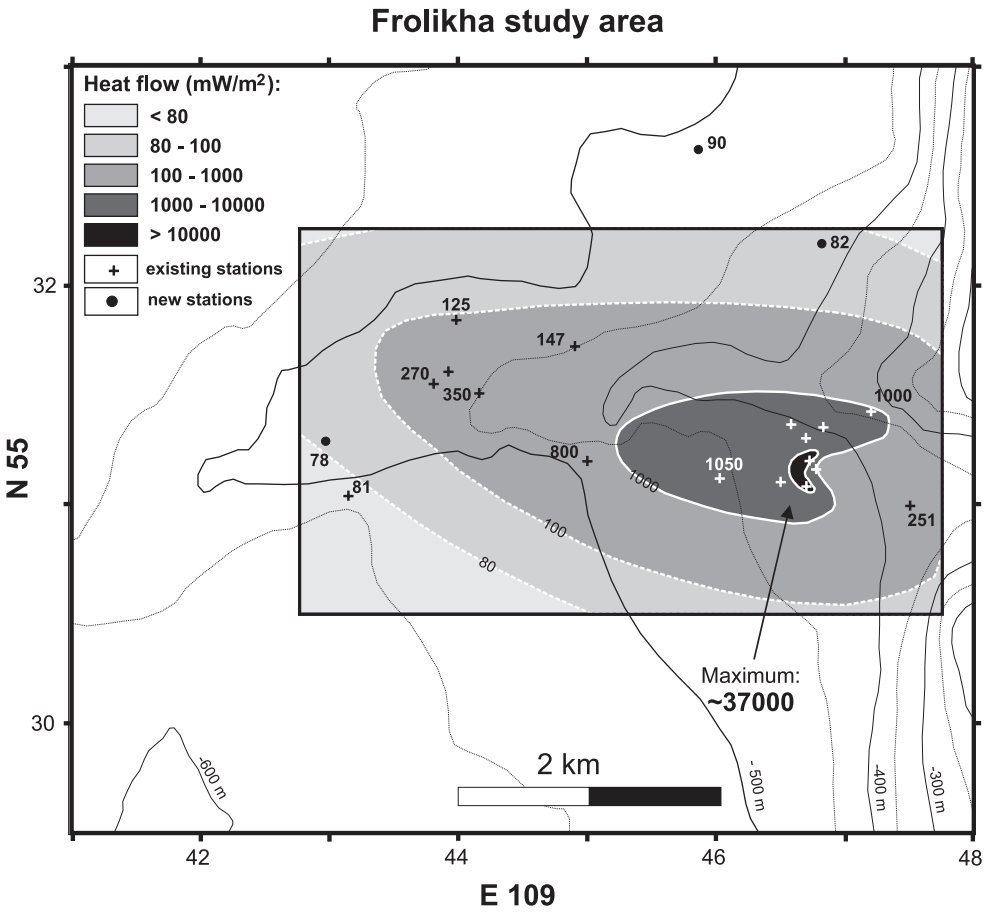

Fig. 5. Heat flow contour map in the Frolikha area, based on existing stations (Golubev, 1982, Crane et al., 1991; Golubev et al., 1993; and previously unpublished data) and new geothermal stations.

error in the station positioning of earlier measurements. The contours of 1000 and 100 mW/m^2 are well constrained on the inner side and show that the anomaly extends for a few kilometers to the west–northwest of the vent center. The contours of 100 mW/m^2 and 80 mW/m^2 have a diameter of 2–4 km and 3–6 km, and suggest a transition to the background heat flow similar to the Zavorotny anomaly.

While the source of the anomaly is obviously related to the hydrothermal venting, the full nature of the anomaly needs to be further defined. The heat flow anomaly is not aligned according to the subaqueous morphological high. This independence suggests a relation with deeper buried tectonic structures, but at this moment no geophysical data exist that can verify such a relation.

5.3. The Hakusy anomaly

The Hakusy study area displays a similar setting as Frolikha, also featuring a single-levee morphological high perpendicular to the coast. Twenty-eight new stations were made (Table 1), concentrically spread around the high heat flow of 2066 mW/m^2. Sediments in the study area allowed good probe penetration and most stations returned near linear thermal gradients.

The grid of geothermal stations allowed to contour in detail the heat flow anomaly offshore Hakusy (Fig. 6). Contouring was performed manually. Surrounding the maximum heat flow of 2066 mW/m^2 (Golubev, 1995), close-spaced contours of 500 to 50 mW/m^2 delimit the anomaly. Outside the study area, stations with gradients smaller than 60–70 mW/m^2 strongly

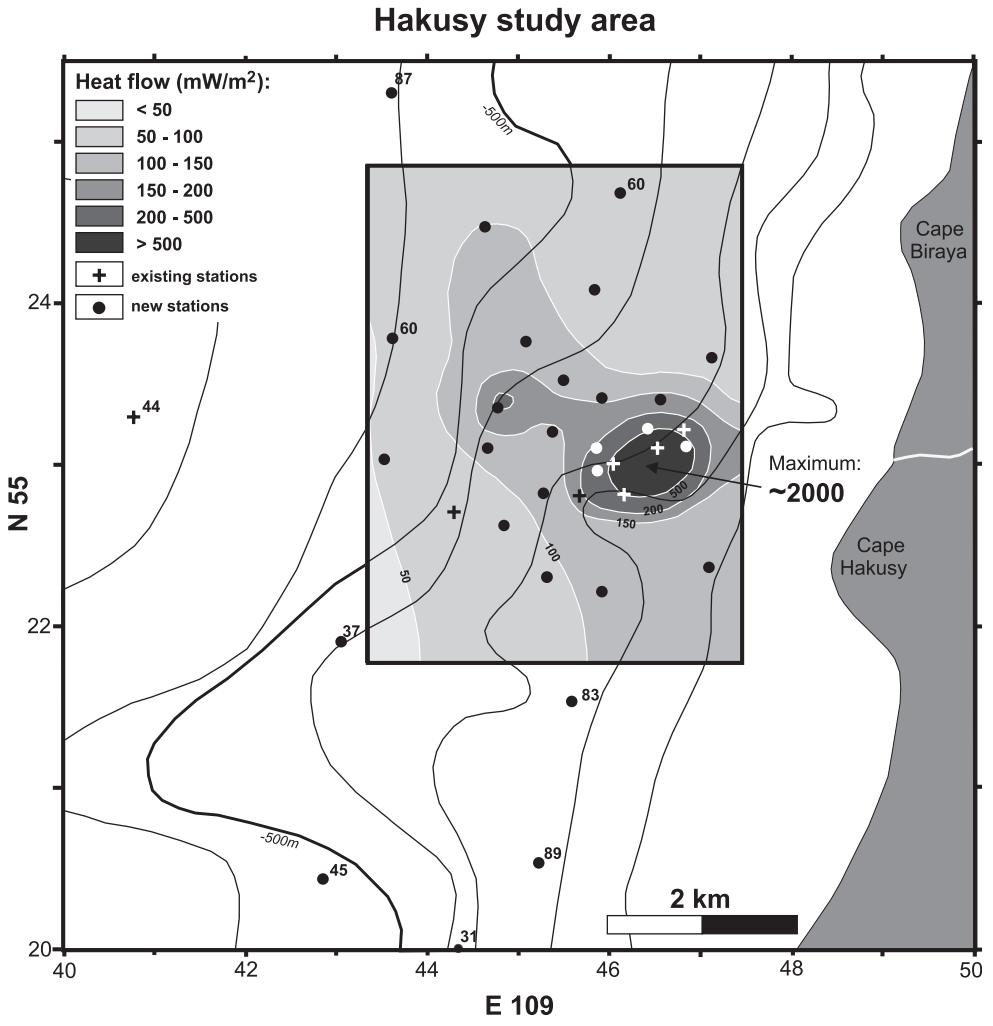

Fig. 6. Heat flow contour map in the Hakusy area, based on existing stations (Golubev, 1982, 1995) and new geothermal stations.

delimit the anomaly to the west and the north. To the south and the east, the 100-mW/m^2 contour is not well constrained due to too shallow water depths preventing accurate heat flow measuring.

The Hakusy surface heat flow expression appears to be slightly smaller than the Frolikha anomaly. Transition to background values as low as 50 mW/m^2 occurs already at 3 km from the center of the anomaly. Strong similarity with Frolikha is found in shape and setting of the anomaly. The shape reveals an east–west direction, slightly turning northwards to the west. A few stations measured on the small sub aqueous high suggest that the anomaly crosses this sedimentary ridge.

5.4. Heat flow anomalies on the Academician Ridge

The Academician Ridge study area has a complete different setting than the previous discussed areas. This ridge is a large transverse zone (25 by 70 km) and bathymetrical high at 300–500-m water depth. The central part exists of two longitudinal sub-ridges with a depression in between. One of the sub-ridges flattens out to the south–west in some kind of a canyon at half-length of the ridge. A total of 38 new geothermal stations (Table 1) were added to the 10 stations previously reported (Golubev, 1982, 1987) and enabled to lay out and contour the moderate heat flow anomalies.

On the heat flow map constructed with intervals of 10 mW/m^2, several geothermal areas can be recognized (Fig. 7). In general, heat flow is slightly elevated with respect to the background heat flow of the NNB (~ 70–90 mW/m^2). More anomalous heat flow is found between the two sub-ridges and in the so-called canyon. Between the two sub-ridges, a thermal anomaly is mapped of 5–7 km in diameter and with a maximum measured heat flow of 120 mW/m^2. Another spot of increased heat flow is found at the tip of the canyon and also on the steep southern slope, a higher heat flow of about 110 mW/m^2 is measured.

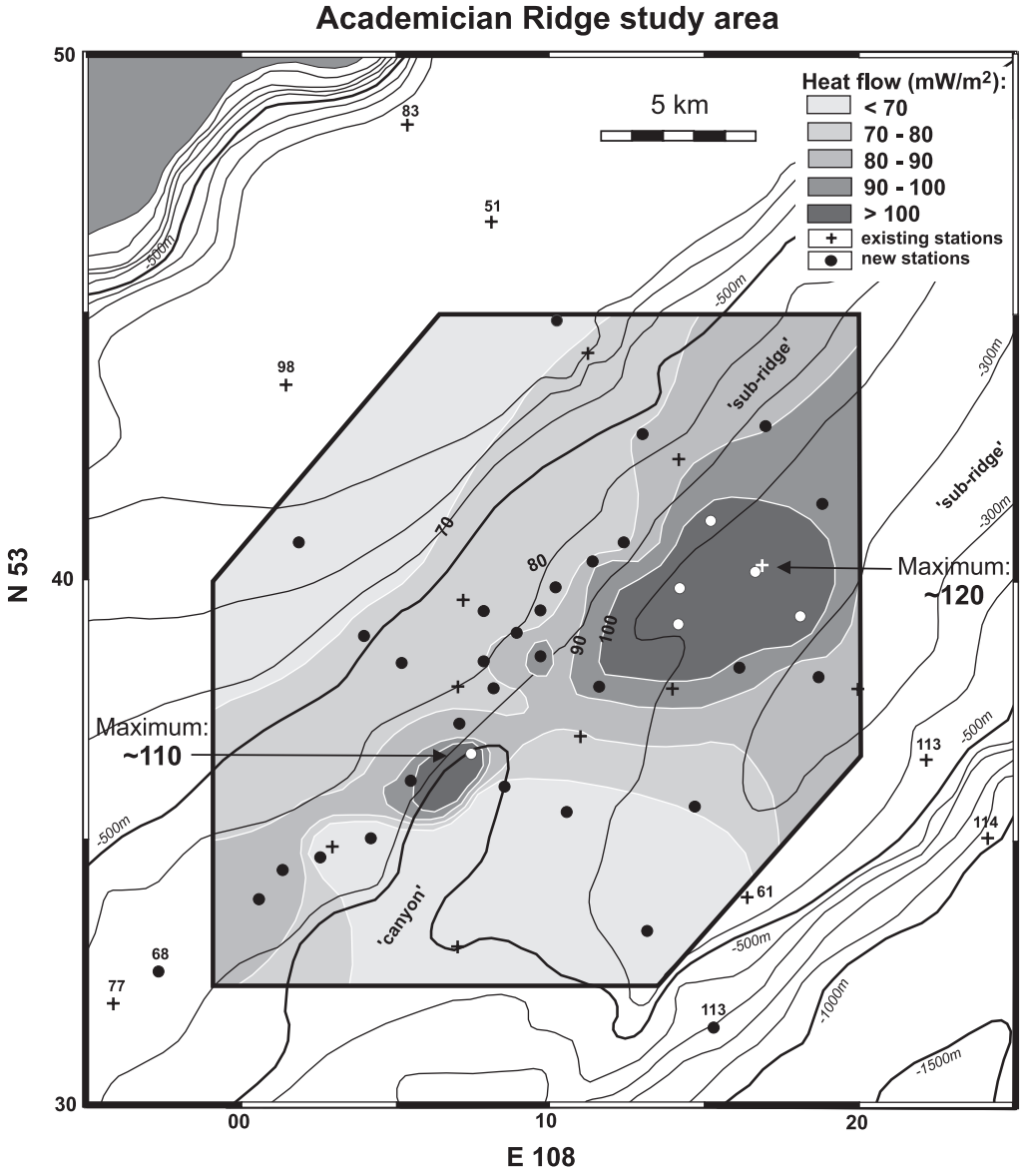

Fig. 7. Heat flow contour map of the study area on Academician Ridge, based on existing stations (Golubev, 1982, 1987) and new geothermal stations. Isobaths are at 100-m intervals.

In the canyon and downslope to the southwest, heat flow decreases over a broad area to values of only 50–60 mW/m^2.

The heat flow anomalies observed on the Academician Ridge have a completely different surface expression compared to the strong, local heat flow anomalies that have been observed along the borders of the NNB. They are rather small heat flow variations with a spatial distribution that suggests a close relation with the structural features of the ridge.

5.5. Heat flow variations along the North Basin axial profile

The NBB is approximately 450 km long and 850–880 m deep along its north–south axis. No strong heat flow anomalies exist in this basin plain, and the heat flow attains the typical background value of 50–70 mW/m^2. It was questioned if a particular variability pattern exists within this 20-mW/m^2 range. To clarify this, a total of 25 new geothermal stations have been performed along an axial profile and at intervals of 5–15 km (Table 1). Along the trans-section, 11 existing stations were crossed (Golubev, 1982).

The new and old heat flow stations together coherently describe variations in the background heat flow and show more details than revealed by the old data only (Fig. 8). In most parts, heat flow is around 60 mW/m^2, but three zones with an elevated heat flow occur at distances of 130 km from each other. Both heat flow intensity (70–80 mW/m^2) and width of the anomalous zones (50–100 km) increase towards the north. At the northern and southern terminations of the axial profile, the heat flow increases sharply from 60 mW/m^2 to values of more than 80 mW/m^2. The regular large-scale pattern in the variability of the background heat flow indicates that their occurrence is not random, but strong indications for a sedimentary or structural control do not exist. Transverse faults crossing the NBB from the western to the eastern border have been proposed (Levi et al., 1982), but strong evidence is lacking.

5.6. Common features of the heat flow anomalies

The new heat flow density investigation in five study areas in the NBB has recognized new features of known heat flow variations. A first type of heat flow anomalies occurs on the flanks of the lake basin and is characterized by heat flow values 5 to 500 times the background heat flow. Detailed mapping showed that all of them are isolated heat flow anomalies extending over distances of only 3–6 km. They are more or less concentric in shape, with a maximum

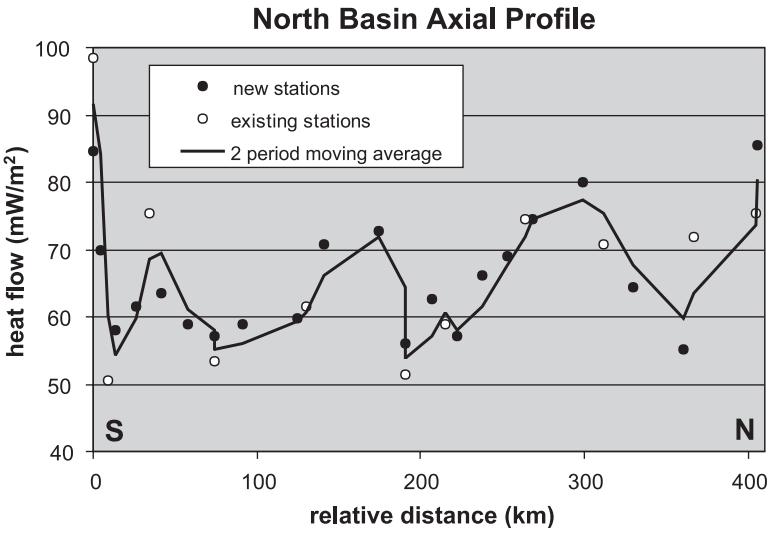

Fig. 8. Heat flow variations along an axial profile in the NBB (see Fig. 2). The existing stations are from Golubev (1982); they were recalculated with an average conductivity of 0.92 W/m K.

heat flow in the center and a sharp decrease away of the center towards the background heat flow of 50–70 mW/m^2. On Academician Ridge, another type of heat flow variations is mapped. Heat flow in this transverse zone bordering the NBB to the south is slightly higher than the basin background: it generally varies between 70 and 90 mW/m^2, and all measured heat flow data fall in the range of 50–120 mW/m^2. Finally, non-random heat flow variations are also outlined within the background heat flow in the basin plain. A heat flow variability with a wavelength of around 110–130 km is observed along the axis of the NNB.

All observed anomalies appear to be more or less structurally controlled. In the Zavorotny study area, the anomalies are all found with a relay-ramp formed by two overstepping border faults and on the eastern side, all anomalies are located opposite river valleys that are probably aligned along transverse faults (Golubev et al., 1993). In Frolikha, it is known that the heat flow anomaly is related to hydrothermal venting on the lake bottom. Considering the similarity with Frolikha, it is suspected that upflowing and discharging fluids play an important role in the other anomalies too. CTD-measurements have shown a small increase of the near bottom-water temperature in the Hakusy anomaly, but at the Zavorotny anomalies no indication of venting was found. The possible mechanism responsible for the strong local anomalies at the east and west borders of the lake will be further analyzed in the next section. A study of the source and nature of the heat flow variations in the basin plain and on Academician Ridge is not be considered here, but all mapped anomalies will be taken into account to estimate their importance in the global basin heat output.

6. Discussion

6.1. Source of heat flow anomalies

6.1.1. Basin fluid flow

The presence of 70 thermal springs in the rift zone, with 10 of them on the shores of northern Lake Baikal and one at the lake bottom, forms a strong evidence for a hydrothermal circulation system in the upper crust. Inferences from mineralisation and isotopic composition suggest that the thermal waters are part of a circulation system with young meteoric water involved and circulating to depth of about 3–5 km (Golubev, 1982). Continental low-temperature systems (<150 °C) as in Baikal, typically involve the downward circulation of cold meteoric water at high elevation, heating of the waters at depth and discharge at lower elevations. These systems are driven by topography and require an elevation gradient in the water table. Steep topographic gradients are present in the Baikal area, particularly in the northern basin that is surrounded by high mountain flanks. Drilling wells at different elevations on the basin flanks indicate a water table close to the surface (Pinneker et al., 1968). A modelling study of the regional heat and fluid circulation by groundwater has shown that such a system is possible during rift evolution and capable of redistributing important quantities of heat towards the basin (Poort and Polyansky, 2002).

It may be assumed that the heat flow anomalies at the bottom of the lake could be simply formed within this regional-scale fluid circulation model. However, within the sedimentary basin, fluid flow is also driven by another independent system. Fluids are percolating through the sediments as a result of the consolidation of the sediments: i.e., compaction-driven fluid flow. The fluids can be leaking in permeable strata and discharge in disturbed and weakened zones. In general, fluid velocities resulting from compaction are not large enough to seriously disturb the thermal field, although a strong anisotropy in the permeability structure of the basin can locally focus the flow.

The considerations above demonstrate that the mapped heat flow anomalies in the NBB can be the result of heat transfer coupled with a complex interaction of local (basin) and regional fluid flow systems. Moreover, the origin and nature of all the recognized lake-based anomalies do not have to be similar. Within the framework of a conceptual model, several aspects of these complex systems can be analyzed quantitatively.

6.1.2. Constraints from fracture model

In a order to quantify the relation between fluid flow and the local surface heat flow anomalies in the Baikal sediments, we will adopt a fracture model suggesting that fluids in the sediments are mainly circulating through a number of individual fractures and openings. The existence of hydrothermal springs

requires heterogeneous permeability where the fluid flow is channelized through high-permeability pathways as open fractures and faults. In order to obtain an analytical solution of a single-phase fluid flow, simple geometries and simple boundary conditions have to be considered. Available analytical solutions in literature generally concentrate on the temperature of the outflowing fluid (Bodvarsson and Lowell, 1972; Turcotte and Schubert, 1982; Deloule and Turcotte, 1989), and indicate the importance of the width and length of the adopted fracture. Golubev (1990) applied the solution of Ziagos and Blackwell (1986) to a rectangular channelized flow circulation in the Baikal rift. This model suggests that the fluid can discharge with a high temperature for a duration of 100–1000 years depending on the flow.

Using the fracture concept, a simple and straight forward approach by Williams et al. (1979) gives a two-dimensional analytical solution for the temperature distribution in the surrounding rocks. A vertical fracture geometry is adopted in a slab bounded by an isothermal lower reservoir (overpressured aquifer) and a shallower isothermal surface (Fig. 9). It is suggested that at the fracture, outflow temperature is increased, and within the fracture, a steady-state flow exists that imposes a steeper linear thermal gradient on the background gradient. Lateral heat loss to the adjacent rock mass will cause sloping isotherms and elevated heat flow around the vent. The boundary conditions of this problem allow to solve the Laplace equation analytically and fluid dynamics equations can be omitted. The surface heat flow q_{surf} is then described as (Williams et al., 1979):

$$q_{surf} = \frac{kT_L}{L}\left(1 + \frac{2T_V}{T_L(e^{\pi y/L} - 1)}\right)$$

where T_L is the temperature at the lower boundary, T_V is the temperature at the venting output (elsewhere temperature is zero at surface), L is the length of the fracture, k is the thermal conductivity, and y is the horizontal distance at the surface away from the venting center. It should be noted that according to numerical modelling results of Pederson and Bjorlykke (1994), the gradient in an upflowing fluid along a fracture stays close to the geothermal gradient and will only decrease, as suggested here, when fluid velocities of more than 100 m/year exist.

6.1.3. Application to Baikal anomalies

The concentric expression of the surface heat flow in northern Baikal anomalies suggests that it is appropriate to apply a discrete model of fluids flowing upwards along a fracture. Using the shape of the detailed heat flow contours as a constraint, the above-stated model and equation can help to make an estimation of the formation depth, the temperature of the venting fluid and the increased (linear) gradient in the upflowing fluid. A background heat flow of 55 mW/m^2 and a thermal conductivity of 2 mW/m^2 are assumed. The most detailed heat flow contours we have are for the Zavorotny anomaly, and a transect is presented in Fig. 9. The model predicts a close fit to this transect for a formation depth of 4.5 km (formation temperature 250 °C) and a venting temperature of 40 °C. A clear misfit is given for venting temperatures by 20 °C smaller or larger, and for a formation depth of 1 km. In fact, the heat flow geometry is not much dependent of the formation depth, and for all depths larger than 2 km, a reasonable shape is predicted. Transects of the Hakusy and Frolikha heat flow anomalies, where contours are not so detailed, suggest a fracture model with significantly different parameters than in northern Zavorotny. The best-fit curves suggest a venting temperature as large as the formation temperature for both anomalies, implying a zero gradient in the upflowing fluid. For the Hakusy anomaly, the predicted formation depth is 2 km ($T_L = T_V = 110$ °C), while for the Frolikha anomaly, the depth is as large as 5 km ($T_L = T_V = 275$ °C). Where in Zavorotny, an infinitely small fracture width is suggested, for Hakusy and Frolikha the steeper gradient in the model had to be shifted by about 100 m from the center to obtain reasonable fits.

The applied fracture model is for sure far too simple to describe the real complexity and geometry of the venting systems active in the northern Baikal. However, the predicted shape of the surface heat flow is close to those of the observed anomalies. This suggests a reasonable first order approximation of the proposed model. Moreover, the modelled formation depth of at least 2 km for all considered anomalies is in good agreement with estimates based on the mineralisation of venting sites on the shores of northern Baikal (Golubev, 1982). The prediction of

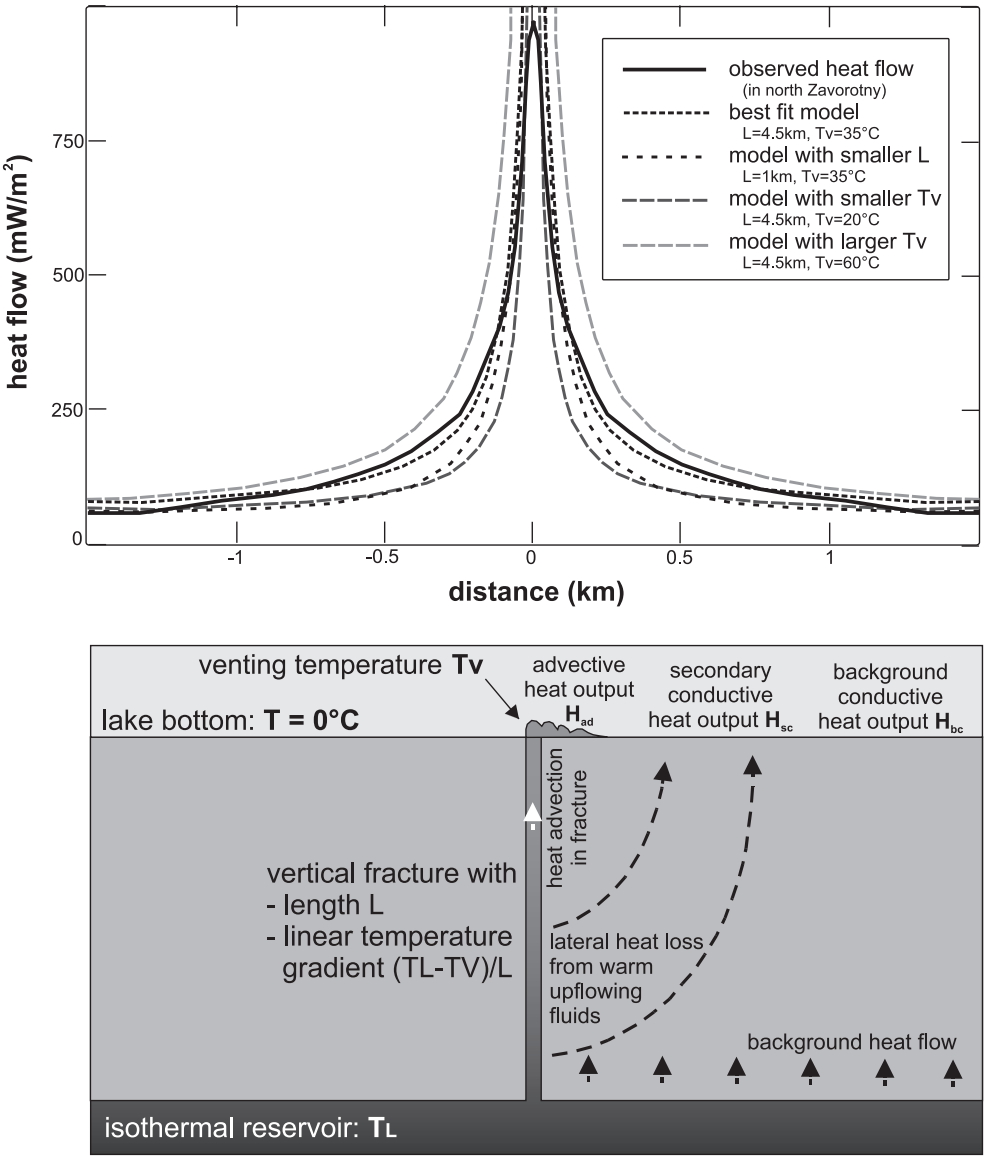

Fig. 9. The fracture model simulating vertical fluid upflow along a fracture and the shape of the heat flow distribution at the surface for different parameter values. The best fit for the Zavorotny heat flow anomaly is shown. At the right side of the fracture model cartoon, the different components of heat output considered at the heat flow anomalies are illustrated.

venting temperature (or temperature close to the surface) as large as the formation temperature for the Frolikha and Hakusy anomaly demands that large upflow velocities exist. In the Zavorotny anomaly on the western side of the lake, upflow is apparently slower, but still large enough to result in a steepened gradient.

6.2. Importance to regional budget

6.2.1. Quantification of heat output

The surface expression of the heat flow anomalies can be described as concentrical patches of elevated heat flow embedded in a more or less uniform background heat flow of 50–70 mW/m^2. In a first

simplification, the background heat flow can be assumed as the purely conductive and stationary result of mantle heat flow and deep crustal heat sources. Within heat flow anomalies, additional heat is transported to the surface. The concentric shape of the heat flow contours with a central heat flow maximum can be reasonable explained in a model with upflowing warm fluids along a vertical channel (see previous section). This model involves a strongly focused heat advection. The heat flow measured by the probing technique and indicated by the contours is, however, conduction heat flow only. The anomalous heat flow must be attributed to a secondary effect of the advective heat process, which is explained in the model as lateral heat loss from the warm upflowing fluids (Fig. 9).

Thus, the total heat output at the anomalies, H_{an}, constitutes of three components:

$$H_{an} = H_{bc} + H_{ad} + H_{sc}$$

where H_{bc} is the background conductive heat output that is present everywhere, H_{ad} is the advective heat output within the fracture, and H_{sc} is the secondary conductive heat output that decreases away from the fracture. The sum $H_{ad}+H_{sc}$ is the additional heat output (H_{ex}) at the anomaly due to the hydrothermal process.

The two conductive components, $H_{bc}+H_{ad}$, can be directly quantified from heat flow measurements and mapping. Only H_{ad} is not directly measured and must be estimated from hydrological data combined with a conceptual model. The adopted fracture model assumes that the outflow of fluids is restricted to a discrete, almost pointed, site of venting. If the temperature of the venting fluid T_V and the amount of discharging fluids Q_S are known, then the advective heat output is given by:

$$H_{ad} = c_p\ \rho\ Q_S(T_V - T_S)$$

where c_p and ρ are the heat capacity and the density of the outflowing fluids, and T_S is the ambient surface temperature. The model assumes that, outside the venting opening, no heat is lost advectively or convectively. If fluids are discharged in a broader area and in a more diffuse sense, the heat advected with it must be strongly limited locally. Available techniques do not allow to quantify the possible total output over a broader region. As convection cells will induce a different surface (conductive) heat flow signal than that observed, it can be assumed that fluid convection and associated convective heat loss are not significant.

6.2.2. Heat output at individual anomalies

On the basis of the detailed heat flow mapping of the offshore thermal anomalies, a good estimate of the conductive heat output in these anomalies is available. In Table 2, for each investigated anomaly, the amount of extra heat loss above several reference heat flow levels is listed. These reference levels can be taken as arbitrary background heat flows. As the background heat flow is somewhere between 55 and 70 mW/m^2, the extra, secondary conductive heat output H_{sc} resulting from the lateral heat loss of the upflowing fluid, must be in the range listed in the first two columns.

Specific features can be recognized for the extra conductive heat output at the different anomalies. For the local anomalies, the extra heat output is obviously the largest at Frolikha, being three to six times larger than in the Hakusy and the Zavorotny anomalies, and

Table 2
Estimated extra conductive heat output for all contoured anomalies and for two different heat flow reference levels

		>55 mW/m^2		>70 mW/m^2		
		Area (km^2)	H_{sc} (MW)	Area (km^2)	H_{sc} (MW)	H_{sc}/H_{bc}
Frolikha anomaly		–	–	19.1	8.1	5.8
Hakusy anomaly		23.8	1.7	18.3	1.4	1.1
Zavorotny anomalies	northern	74.2	2.9	59.8	1.9	0.5
	central	13.5	0.7	9.6	0.5	0.7
	southern	23.1	1.4	18.4	1.1	0.8
Academecian anomalies	eastern	–	–	191.5	3.4	
	western	–	–	25	0.4	

Also listed is the area over which the extra output occurs.

even more than the sum of all the others. Almost all of this output is attributed to heat flow levels higher than 150 mW/m^2; heat output between that level and the background heat flow is similar for all main anomalies. The northern Zavorotny anomaly, on the other hand, differs from the others by its considerably larger area over which the extra output occurs. The quotient of the extra heat output H_{sc} to the background output H_{bc} is probably the best parameter that demonstrates the differences between the anomalies. This value is generally around 1, but ranges from only 0.5 in northern Zavorotny to more than 5 in Frolikha. Moreover, the anomalies along the western side of the northern Baikal Basin all have a quotient smaller than 1, and anomalies on eastern side larger than 1. These differences could be attributed to different fracture geometries and upflowing parameters, as has been demonstrated in the analogue modeling section. The anomalies on the Academician Ridge are different from the local anomalies as they do not fit the fracture model. However, their contours do allow to estimate the extra conductive heat output, which is listed in Table 2.

The direct advective heat output component at the offshore local anomalies is not well constrained. The temperature and the rate of the discharging fluids are the main parameters needed, but they are difficult to measure in the relatively deep offshore anomalies. Moreover, only at Frolikha, it has been proven that water is actually venting at the lake bottom. A temperature of 16 °C has been measured in the vent center (Crane et al., 1991). Estimates of the rate of fluid discharge do not exist for the Frolikha offshore vent. On the other hand, the fluid discharge has been measured for all seven springs on the shores of northern Baikal and averages to about 10 l/s. It is reasonable to adopt this discharge for the offshore Frolikha vent too. The same rate is obtained if we multiply the discharge velocity, as estimated in the analogue modelling section, with a reasonable vent width of 100 m. Using the above-stated formula, the advective heat output H_{ad} for the Frolikha anomaly is estimated at 0.5 MW. For the other local thermal anomalies, we will assume the same amount of advective heat output. Considering the conclusions from the analytical modelling and the fact that all anomalies have a smaller maximum heat flow than the Frolikha one, this is probably an overestimation.

6.2.3. Total heat output in the northern basin

To make the balance of the total extra heat output in the northern Lake Baikal Basin, all known local thermal anomalies have to be considered. For the sites not investigated in detail—Tompuda, Shegnanda, Davsha and Baikalskoe—data are insufficient to quantify the secondary conductive output. For these anomalies, we will assume the same value of extra heat output estimated for Hakusy and northern Zavorotny. The estimates for the secondary conductive and the advective heat output of these sites are an upper limit. On the other hand, it is not sure that all anomalies have been detected, and therefore, some of the extra output may not have been included. With the estimation of a heat loss at all individual anomalies based on the assumption of a venting model, a total extra heat output in the northern Baikal of about 20–25 MW is calculated (Table 3). The direct advective output contributes for 30%, but the largest part is lost conductively near the vent center due to lateral heat loss of the upflowing fluid.

If we assume that the heat flow prior to rifting was uniformly at a level of 55–70 mW/m^2, which is the range for a background heat flow in an orogenically altered crust, the known heat flow anomalies do not have increased the heat output by more than 5%. Averaged over the whole region of the northern Lake Baikal Basin (about 13000 km^2), this converts to a uniform elevation of the background heat flow by 3 mW/m^2.

6.2.4. Heat source

The extra heat brought to the surface is minimal if considered as a ‘measurable’ averaged heat flow increase at the surface of the basin, but it is a

Table 3
The total extra heat output at the anomalies relative to the total background heat output in the North Baikal Basin

	For a background heat flow of 55 mW/m^2 (MW)	For a background heat flow of 70 mW/m^2 (MW)
Total H_{bc}	715.0	910.0
Total H_{ex}	28.3	23.6
Total H_{ad}	24.3	19.6
Total H_{sc}	4.0	4.0
Total H_{nb}	743.3	933.6
Total H_{ex}/H_{bc} (in %)	4.0	2.6

See text for explanation of abbreviations.

significant amount of heat that requires a heat source. It has been shown (Poort and Polyansky, 2002) that heat can be redistributed by the regional fluid circulation, and that the heat output is increased over the basin and decreased over the uplifted flanks. The balance of the two is positive with an extra output over the basin that has a proportion of 2–10% to the background. The largest part of the extra heat lost at the surface is brought up from beneath the basin, and a minor part is transferred from the flanks.

Does the absence of a strong, regional heat flow anomaly at the surface not contradict with the deep rifting processes in Baikal? A kinematic model of extension, employed to assess the deep lithospheric structure and associated thermal perturbation across the Baikal rift, showed that the surface thermal expression is not representative for the deeper thermal structure of the rifted lithosphere (Poort et al., 1998). It was suggested that a possible asthenospheric upwarp is more likely to be situated below the northern than below the central Baikal Basin, but none of the models predicts a significant (>10 mW/m^2) increase in regional surface heat flow. For deep heat to escape rapidly at the surface, additional processes like deep fluid convection or magmatic intrusions are needed to bring it up from lower crustal levels. A recent dynamic modeling study of the lithospheric-scale deformation in the north Baikal rift (Lesne et al., 2000) suggests that the rifted lithosphere is only hydrostatically supported by the asthenosphere, without input of additional thermal or mechanical energy.

7. Conclusion

Detailed mapping of high heat flow anomalies on both sides of the North Baikal Basin showed that they are of local character only, not extending for more than 4 km in diameter. The maximum measured heat flow reaches values of 0.3–35 W/m^2, which decrease logarithmically in all directions to background values of 50–70 mW/m^2. This background heat flow is measured in the major part of the northern basin and appears to fluctuate in a north–south direction along a long-wavelength of 250 m. There is an additional tendency of higher heat flow intensity towards the north for both the background heat flow and the thermal anomalies. At the northern and southern termination of the basin, heat flow is moderately elevated, with maxima around 90–120 mW/m^2 and with a strong variation in the shape and extent of the anomalies.

The small extent of the strong, local anomalies excludes a conductive source, and fitting the surface heat flow expressions to a fracture flow model suggests that warm-fluid flow along a linear fault is a reasonable source mechanism. Presently, only in the Frolikha anomaly, it is proven that the heat flow anomaly is connected to hydrothermal outflow on the bottom of the lake. The required strong upflow of fluids in the basin can be supported by a regional flow system from the uplifted rift flanks. The outlined thermal anomalies are all of a positive signature and a quantification of the extra heat output is made considering two components: secondary conductive and advective heat loss. The wall rock conductive output is directly quantified from the detailed contouring of the surface heat flow anomalies, and amounts to 20 MW in total for all known anomalies. The advective component is estimated to be 3.5 MW offshore using the parameters of the Frolikha hydrothermal vent, and 13 MW for on-shore vents. Relative to a basal heat flow of 55–65 mW/m^2, these estimations suggest an extra heat output in the northern Lake Baikal of only 5%, corresponding to a regional heat flow increase of 3 mW/m^2.

The surface heat flow pattern surveyed in the Baikal Basins is a result of fluid circulation processes on a basin-scale. Besides these variations, the surface heat flow is not expected to bear a signal of deeper lithospheric thermal anomalies that can be separated from heat flow typical for orogenically altered crust (40–70 mW/m^2). Not the elevated heat flow is a typical feature of the rift, but the existence of heat flow variations with strong local anomalies. The absence of a regional heat flow anomaly does not correspond to the classical view of continental rifts. In the classical continental rifts, such as the Kenya rift, heat flow is much more elevated regionally. The Baikal rift has been considered a-typical for other rifting features too, such as the absence of strong crustal thinning, deep seismicity and a significant mechanical strength of the lithosphere. The new insights on the geothermal signature in the Baikal rift once more show that the typical description of a continental rift has to be revised thoroughly. Rifting is not by default synonymous to high heat flow.

Acknowledgements

J. Poort has a post-doctoral fellowship from the Fund for Scientific Research—Flanders (FWO). We are greatly indebted to V. Golubev for his collaboration in the acquisition of the data and the discussion of the scientific results. We thank M. Rubtsov and his PALS-team from Samara for their support in employing the GEOS thermoprobe, and M. Grachev, O. Khlystov and N. Granin for the logistic support, and the captain and crew of R.V. Titov for their craftsmanship.

References

Back, S., De Batist, M., Strecker, M.R., Vanhauwaert, P., 1999. Quaternary depositional systems in Northern Lake Baikal. Siberian J. Geol. 107, 1–12.

Bodvarsson, G., Lowell, R.P., 1972. Ocean-floor heat flow and the circulation of intersticial waters. J. Geophys. Res. 77, 4472–4475.

Burov, E.B., Houdry, F., Diament, M., Déverchère, J., 1994. A broken plate beneath the North Baikal rift zone revealed by gravity modelling. Geophys. Res. Lett. 21, 129–132.

Colman, S.M., Jones, G.A., Meyer Rubin, King, J.W., Peck, J.A., Orem, W.H., 1996. AMS Radiocarbon analyses from Lake Baikal, Siberia: challenges of dating sediments from a large, oligotropic lake. Quat. Sci. Rev. (Quat. Geochron.) 15, 669–684.

Colman, S.M., Karabanov, E.B., Nelson, C.H., 1998. Quaternary depositional patterns and environments in Lake Baikal from high-resolution seismic stratigraphy and coring. In: Mats, D.R., Hutchinson, D.R. (Eds.), Baikal Rift in the Cenozoic. Cambridge Univ. Press, London.

Crane, K., Hecker, B., Golubev, V.A., 1991. Heat flow and hydrothermal vents in lake Baikal, U.S.S.R. Eos, Transactions, AGU 72, 1–6.

Davis, E.E., Seemann, D.A., 1994. Anisotropic thermal conductivity of Pleistocene turbidite sediments of the northern Juan de Fuca Ridge. Proc. Ocean Drill. Program Sci. Results 139, 559–565.

Deloule, E., Turcotte, D.L., 1989. The flow of hot brines in cracks and the formation of ore deposits. Econ. Geol. 84, 2217–2225.

Delvaux, D., Fronhoffs, A., Hus, R., Poort, J., 2000. Normal faults splays, relay ramps and transfer zones in the Central Parts of the Baikal rift basins: insights from digital topography and bathymetry. Bull. Cent. Rech. Explor. Prod. Elf-Aquitaine 22, 2–20.

Déverchère, J., Houdry, F., Solonenko, N.V., Solonenko, A.V., Sankov, V.A., 1993. Seismicity, active faults and stress field of the North Muya region, Baikal rift: new insights on the rheology of extended continental lithosphere. J. Geophys. Res. 98, 19895–19912.

Duchkov, A.D., Kazantsev, S.A., Golubuv, V.A., Lysak, S.V., Khaikovskii, E.S., 1976. The heat flow within Lake Baikal. Sov. Geol. Geophys. 17, 92–99.

Duchkov, A.D., Kazantsev, S.A., Velinskii, V.V., 1979. Heat flow of Lake Baikal. Sov. Geol. Geophys. 20, 110–113.

Duchkov, A.D., Lysak, S.V., Golubev, V.A., Dorofeeva, R.P., Sokolova, L.S., 1999. Heat flow and geothermal field of the Baikal Region. Russ. Geol. Geophys. 40, 289–304.

Edgington, D.N., Klump, J.V., Robbins, J.A., Kusner, Yu.S., Pampura, V.D., Sandimirov, I.V., 1991. Sedimentation rates, residence times and radionuclide inventories in Lake Baikal from 137Cs and 210Pb in sediment cores. Nature 350, 601–604.

Golmshtok, A.Y., Duchkov, A.D., Hutchinson, D.R., Khanukaev, S.B., 2000. Heat flow and gas hydrates of the Baikal Rift Zone. Int. J. Earth Sci. 89, 193–211.

Golubev, V.A., 1978. Geothermal investigations on Lake Baikal using a cable probe-thermometer. Izv., Earth Phys. 14, 235–238.

Golubev, V.A., 1982. Geothermics of Baikal Nauka, Novosibirsk. 150 pp. (in Russian).

Golubev, V.A., 1984. Recognition of underwater hydrotherms in Baikal by a method of near-bottom profiling. Izv., Earth Phys. 20, 104–107.

Golubev, V.A., 1987. Geothermal and hydrothermal studies on Middle Baikal. Izv., Earth Phys. 7, 14–26.

Golubev, V.A., 1990. Hydrothermal systems, permeability, and thermal models of the crust in the Baikal rift zone. Izv., Earth Phys. 26, 916–924.

Golubev, V.A., 1995. Hydrothermal vents in Lake Baikal and the heat balance of the lake. Trans. (Dokl.) Russ. Acad. Sci. Earth Sci. Sect. 328, 27–32.

Golubev, V.A., 2000. Conductive and convective heat flow in the bottom of Lake Baikal and in the surrounding mountains. Bull. Cent. Rech. Explor. Prod. Elf-Aquitaine 22, 323–340.

Golubev, V.A., Osokina, S.V., 1980. Distribution of heat flux and nature of local anomalies in Baïkal lake region. Izv., Earth Phys. 16, 265–272.

Golubev, V.A., Poort, J., 1995. Local heat flow anomalies along the western shore of north Baikal basin (Zavorotny area). Russ. Geol. Geophys. 36, 174–185.

Golubev, V.A., Klerkx, J., Kipfer, R., 1993. Heat flow, hydrothermal vents and static stability of discharging thermal water in lake Baikal (southeastern Siberia). Bull. Cent. Rech. Explor. Prod. Elf-Aquitaine 17, 53–65.

Hohmann, R., Kipfer, R., Peeters, F., Piepke, G., Imboden, D.M., Shimaraev, M.N., 1997. Processes of deep water renewal in Lake Baikal. Limnol. Oceanogr. 42, 841–855.

Hutchinson, D.R., Golmshtok, A.J., Zonenshain, L.P., Moore, T.C., Scholz, C.A., Klitgord, K.D., 1992. Depositional and tectonic framework of the rift basins of Lake Baikal from multichannel seismic data. Geology 20, 589–592.

Jemsek, J., Von Herzen, R., 1989. Measurement of in-situ sediment thermal conductivity: continuous-heating method with outrigged probes. In: Wright, J.A., Louden, K.E. (Eds.), Handbook of Seafloor Heat Flow. CRC Press, Boca Raton, FL, pp. 91–120.

Kipfer, R., Aeschbach-Hertig, W., Hofer, M., Hohmann, R., Imboden, D.M., Bauer, H., Golubev, V., Klerkx, J., 1996. Bottom-water formation due to hydrothermal activity in Frolikha Bay,

Lake Baikal, Eastern Siberia. Geochim. Cosmochim. Acta 60, 961–971.

Lachenbruch, A.H., 1968. Rapid estimation of the topographic disturbance to surficial thermal gradients. Rev. Geophys. 6, 365–400.

Lesne, O., Calais, E., Deverchère, J., Chéry, J., Hassani, R., 2000. Dynamics of intracontinental extension in the north Baikal rift from two-dimensional numerical deformation modeling. J. Geophys. Res. 105 (B9), 21727–21744.

Levi, K.G., Sherman, S.I., Plyusnina, L.V., 1982. Map of neotectonics of the Baikal and Transbaikal territories. In: Logatchev, N.A. (Ed.), Nauka, Institute of the Earth's Crust, Irkutsk.

Lister, C.R.B., 1970. Measurement of in-situ conductivity by means of Bullard-type probe. Geophys. J. R. Astron. Soc. 19, 521–533.

Logatchev, N.A., 1993. History and geodynamics of the Baikal Rift (East Siberia): a review. Bull. Cent. Rech. Explor. Prod. Elf-Aquitaine 17, 353–370.

Lounden, K.E., Wright, J.A., 1989. Marine heat flow data: a new compilation of observations and brief review of its analysis. In: Wright, J.A., Louden, K.E. (Eds.), Handbook of Seafloor Heat Flow. CRC Press, Boca Raton, FL, pp. 3–67.

Louden, K.E., Wallace, D.O., Courtney, R.C., 1987. Heat flow and depth versus age for the Mesozoic northwest Atlantic Ocean: results from the Sohm abyssal plain and implications for the Bermuda Rise. Earth Planet. Sci. Lett. 83, 109–122.

Lubimova, E.A., 1969. Heat flow patterns in Baikal and other rift zones. Tectonophysics 8, 457–467.

Lysak, S.V., 1978. The Baikal rift heat flow. Tectonophysics 45, 87–93.

Lysak, S.V., 1984. Terrestrial heat flow in the south of East Siberia. Tectonophysics 103, 205–215.

Lysak, S.V., 1995. Terrestrial heat and temperatures in the upper crust in South East Siberia. Bull. Cent. Rech. Explor. Prod. Elf-Aquitaine 19, 39–57.

Lyubimova, Ye.A., Shelyagin, V.A., 1966. Heat flow through the bottom of Lake Baikal. Trans. (Dokl.) Russ. Acad. Sci. Earth Sci. Sect. 171, 25–28.

Moore Jr., T.C., Klitgord, K.D., Golmshtok, A.J., Weber, E., 1997. Sedimentation and subsidence patterns in the central and north basins of Lake Baikal from seismic stratigraphy. GSA Bull. 109, 746–766.

Nelson, C.H., Karabanov, E.B., Colman, S.M., 1995. Late Quaternary turbidite systems in Lake Baikal, Russia. In: Pickering, R.N., Hiscott, R.N., Kenyon, N.H., Ricci Luchi, F., Smith, R.D.A. (Eds.), Atlas of Deep Water Environments: Architectural Style in Turbidite Systems. Chapman and Hall, London, pp. 29–33.

Nelson, C.H., Karabanov, E.B, Colman, S.M., Escutia, C., 1999. Tectonic and sediment supply control of deep rift lake turbidite systems; Lake Baikal, Russia. Geology 27, 163–166.

Pederson, T., Bjorlykke, K., 1994. Fluid flow in sedimentary basins: model of pore water flow in a vertical fracture. Basin Res. 6, 1–16.

Pinneker, E.V., Lomonosov, I.S., 1973. On genesis of thermal waters in the Sayan–Baikal highland. Proceedings of Symposium on Hydrogeochemistry and Biogeochemistry. Hydrogeochemistry, vol. 1. Clarke, Washington, pp. 246–253.

Pinneker, E.V., Pisarsky, B.I., Lomonosov, I.S., Koldysheva, R.Ya., Didenko, A.A., Sherman, S.I., 1968. Hydrogeology of Near-Baikal. Nauka, Moscow. 170 pp. (in Russian).

Polyak, B.J., Prasolov, E.M., Tolstikhin, I.N., 1992. He-isotopes in the fluids of the Baikal rift. Izv. Akad. Nauk SSSR, Ser. Geol. 10, 18–33 (in Russian).

Poort, J., 2000. Significance of the surface heat flow in the Baikal Rift: inferences from spatial heat flow analysis and numerical modelling. Ph.D. Thesis, Free University of Brussels (VUB). Brussels. 112 pp.

Poort, J., Polyansky, O., 2002. Heat transport by groundwater flow during the Baikal Rift evolution. Tectonophysics 351 (1–2), 75–89.

Poort, J., Van der Beek, P., Ter Voorde, M., 1998. An integrated modelling study of the central and northern Baikal rift: evidence for non-uniform lithospheric thinning? Tectonophysics 291, 101–122.

Shimaraev, M.N., Granin, N.G., Zhdanov, A.A., 1993. Deep ventilation of Lake Baikal waters due to spring thermal bars. Limnol. Oceanogr. 38 (5), 1068–1072.

Sturm, M., Vologina, E.G., Levina, O.V., Flower, R.J., Ryves, D., Lees, J.A., 1998. Hemipelagic sedimentation and turbidites in the active tectonic basin of Lake Baikal. Conference April 30–May 2 1998, Gent Belgium, Abstract Book. RUG, Gent, pp. 33–34.

Turcotte, D.L., Schubert, G., 1982. Geodynamics; Applications of Continuum Physics to Geological Problems. Wiley, New York. 450 pp.

Von Herzen, R.P., Uyenda, S., 1963. Heat flow through the eastern Pacific ocean floor. J. Geophys. Res. 68, 4219–4251.

Weiss, R.F., Carmack, E.C., Koropalov, V.M., 1991. Deep-water renewal and biological production in Lake Baikal. Nature 349, 665–669.

Williams, D.L., Green, K., van Andel, T.H., Von Herzen, R.P., Dymond, J.R., Crane, K., 1979. The hydrothermal mounds of the Galapagos rift: observations with DSRV Alvin and detailed heat flow studies. J. Geophys. Res. 84, 7467–7484.

Williams, D.F., Kuzmin, M.I., Kawai, T., Khakhaev, B.N., Pevzner, L.A., Karabanov, E.B., Peck, J., King, J., Krachinsky, V., Geletti, V., Kolmnichkov, G., Gvodzkov, A., Prokopenko, A.A., Tsukahara, H., Oberhansli, H., Schwab, M., Weil, D., Grachev, M.A., Khlstov, O., Mandelbaum, A., 1997. Continuous paleoclimate record recovered for last 5 million years. Eos, Transactions 78 (597), 601–604.

Ziagos, J.P., Blackwell, D.D., 1986. A model for the transient temperature effects of horizontal fluid flow in geothermal systems. J. Volcanol. Geotherm. Res. 27, 371–398.

Zonenshain, L.P., Kuzmin, M.I., Natapov, L.M., Page, B.M., 1990. Geology of the USSR: a plate-tectonic synthesis. AGU Geodynamics Series, vol. 21. American Geophysical Union, Washington, DC. 240 pp.